Available online at www.sciencedirect.com

ScienceDirect

Physics of Life Reviews 44 (2023) 279–301

PHYSICS of LIFE reviews

www.elsevier.com/locate/plrev

Review

Mechanotransduction in tumor dynamics modeling

B. Blanco [a,b,*], H. Gomez [c], J. Melchor [b,d,e], R. Palma [a], J. Soler [d,f,**], G. Rus [a,b,d]

[a] *Department of Structural Mechanics, University of Granada, 18071 Granada, Spain*
[b] *Instituto de Investigación Biosanitaria, ibs.GRANADA, 18012 Granada, Spain*
[c] *School of Mechanical Engineering, Purdue University, West Lafayette, IN, 47907, USA*
[d] *Research Unit "Modelling Nature" (MNat), Universidad de Granada, 18071 Granada, Spain*
[e] *Department of Statistics and Operations Research, University of Granada, 18071 Granada, Spain*
[f] *Departamento de Matemática Aplicada, Facultad de Ciencias, Universidad de Granada, 18071 Granada, Spain*

Received 23 January 2023; accepted 30 January 2023
Available online 15 February 2023
Communicated by E. Di Mauro

Abstract

Mechanotherapy is a groundbreaking approach to impact carcinogenesis. Cells sense and respond to mechanical stimuli, translating them into biochemical signals in a process known as mechanotransduction. The impact of stress on tumor growth has been studied in the last three decades, and many papers highlight the role of mechanics as a critical self-inducer of tumor fate at the in vitro and in vivo biological levels. Meanwhile, mathematical models attempt to determine laws to reproduce tumor dynamics.

This review discusses biological mechanotransduction mechanisms and mathematical-biomechanical models together. The aim is to provide a common framework for the different approaches that have emerged in the literature from the perspective of tumor avascularity and to provide insight into emerging mechanotherapies that have attracted interest in recent years.

Keywords: Computational mechanics; LIUS; Mechanotherapy; Mechanotransduction; Tumor dynamics

1. Mechanotransduction in target therapy

The quest to unveil the molecular mechanisms by which mechanical forces modulate signal transduction and gene expression has been raised in the 21^{st} century to understand the mechanisms of cellular responses to the physiological environment [1–6]. Although a large part of the specific responses of the mechanism are being investigated, being currently a hot topic, and are inherent to each type of cell line, in this section, we try to elucidate the main premises that have regulated tumor stress state up to date, outlining an example of the leading hypotheses underlying mechanotherapy.

* Corresponding author at: Department of Structural Mechanics, University of Granada, 18071 Granada, Spain.
** Corresponding author at: Departamento de Matemática Aplicada, Facultad de Ciencias, Universidad de Granada, 18071 Granada, Spain.
E-mail addresses: bblanco@ugr.es (B. Blanco), jsoler@ugr.es (J. Soler).

https://doi.org/10.1016/j.plrev.2023.01.017

Mechanotransduction begins with the transmission of forces to tissue or cellular elements and ends with the integrated response of the cell group [3,7]. The initial mechanical signal – mechanotransmission – occurs locally and is channeled to other mechanosensors along the linked cytoskeleton network extremely fast, on the order of hundreds of milliseconds [7,8]. If the forces are significant and are transmitted for a sufficiently long time, mechanical stimuli cause the deformation of cellular structures that expand and strengthen in response to tension [9]. The conformational changes are followed by the selective triggering of intracellular biochemical signaling events – mechanosensing– [10,11]. Then, the cytoskeletal components and those of the cell membrane are leading mechanisms for helping to transmit a complete set of chemical and physical signals that become a controlled mechanoresponse that regulates the prognostic of the cell [12,13].

The mechanoresponsive pathways integrate the cellular response to force over space and time. The mechanoresponse develops on slower time scales than other signals: transmission signaling pathways occur over minutes, and gene expression pathways can occur from hours to days [7,14]. The leading network of cellular mechanotransduction comprises mainly transmembrane receptor proteins and the cytoskeleton, as well as extracellular matrix (ECM) proteins [6,15]. Several hypotheses aim to explain outside-in mechanotransduction activation and how forces could enhance apoptosis, decrease proliferation, and prevent migration. Since numerous studies detail the extensive biological pathways of mechanotransduction[1] [3,13,16,17], this work focuses only on the core components (Fig. 1) to subsequently understand and propose mathematical frameworks that attempt to model them. We intend to propose how mechanotransduction signaling pathways can be used as a targeted therapy.

- **Transforming Growth Factor β**
  Transforming Growth Factor TGF-β is a family of cytokines that display a dual role in the tumor: at the early stages of the disease, acting as a tumor suppressor inhibiting cell cycle progression, and in advanced stages, promoting the Epithelial to Mesenchymal Transition (EMT), inducing the pro-tumorigenic response [18–21]. The molecular events triggered by TGF-β drive the activation of canonical cascade signaling using SMADs [22], although non-canonical pathways, such as mitogen-activated protein kinase/extracellular signal-regulated (MAPK/ERK), have also been shown to influence tumor progression [23–25]. In later stages, tumor cells avoid the anti-tumorigenic properties of TGF-β through inactivation of TGF-β receptors, SMAD genes, or selective silencing of the properties of apoptotic TGF-β properties [24]. Furthermore, the feedback between ECM remodeling and the TGF-β signaling cascade [26] is critical in tumor control [27]. Experiments demonstrated that soft ECM and increased TGF-β induced apoptosis, while increasing stiffness resulted in EMT employing non-canonical signaling pathways [27–30]. Considering that in advanced disease, increasing the stiffness of the microenvironment ECM promotes tumor invasion and metastasis through the EMT, it clearly states that it is crucial to be aware of the stage at which action is required to regulate TGF-β action.
- **Integrin-focal adhesions**
  Integrins are transmembrane receptors that regulate mainly cell-ECM adhesion. Integrins are activated by responding to the forces exerted by fibronectin alignment and stiffness of the ECM [31]. Once the stimulus is transmitted, the talin and kindlin proteins connect the tail of the integrin to the actin fibers. Focal adhesion is complete with the binding of Focal Adhesion Kinase (FAK) [32,33]. This activation promotes the linkage of vinculin [34–36], which adheres to actin in the cytoskeleton. The regulators of the actin cytoskeleton act downstream of Rho GTPase, triggering the activation of cascade signaling pathways: RHO–associated protein kinase (RHO–ROCK) and phosphatinositide–3–kinase–protein kinase B (P1K3-AKT), which act as pro-oncogenes that induce lamellipodia protrusions, migration, motility, and decreased apoptosis [13,37–40]. Therefore, it is clear that blocking FAK overexpression and the P13K-AKT and RHO / ROCK pathways are therapeutic targets to investigate [41].
- **Wnt- Frizzled**
  Wnt glycoprotein ligands adhere to Frizzled receptor proteins and trigger the modulation of the β-catenin protein and co-receptors [42] through the canonical pathway [43]. This activation involves its translocation to the nucleus, where cell growth, motility, and differentiation are regulated [42,44,45]. In addition, there are noncanonical pathways independent of β-catenin: One of the most relevant pathways in tumor development is Wnt-Ca^{2+} [43,46],

[1] Note that only outside-in and isolation mechanisms are considered here. We assume neither cell-cell interactions nor existing links, which frequently act as hubs for other signaling regulations.

where binding of Wnt to receptors causes a temporary increase in Ca^{2+} concentration. In particular, it is remarkable to point to the rise of cytoplasmatic Ca^{2+} through the Piezo1 ion channel as a promoter of Wnt and P13K-AKT vias [47–51]. Inactivation of Wnt reduces migration by down-regulating the expression of matrix metalloproteinase (MMP) [52–54] and reduces the expression of EMT [54–56]. Furthermore, Wnt inhibitory factors (WIF-1) have also been demonstrated to significantly reduce tumor growth [54,57,58]. Thus, it could be hypothesized that the mechanical stimulus could knock down the Wnt pathway, regulating tumorigenesis and cell invasion.

- **Hippo**
  The Hippo pathway is a highly conserved kinase pathway that regulates cell proliferation, size, migration, and angiogenesis [59–62]. Downstream regulation starts with the NF2 kinase protein and the serine / threonine protein kinases MST1 / 2 and the Large Tumor Suppressor (LATS1 / 2), which activate adapter proteins SAV1 and MOB1 [61,63]. The Hippo pathway suppresses downstream transcriptional coactivators, the Yes-associated protein, and the transcription regulation protein 1 (YAP / TAZ) [64,65], phosphorylates and stores them in the cytoplasm, and inhibits their nuclear transcription [66–68]. The localization of YAP-TAZ in the nucleus is identified as an oncogene that promotes EMT, malignancy, and secondary tumors [60,61]. Nuclear activation of YAP-TAZ is also related to other vias (e.g., PI3K-AKT and Wnt) through high ECM stiffness, heterogeneous cell shape, loss of cell adhesions, and disturbed flow [66,69,70]. Therefore, blocking YAP-TAZ nuclear transcription and regulating the Hippo pathway is critical in mechanotherapy [63,71,72].
- **Hedgehog-Gli (Hh-Gli)**
  Hedgehog proteins (in particular Sonic Hedgehog -SHh-) silence the Patched1 transmembrane protein (PTCH1), relieve Smoothened protein (SMO) and regulate the transcriptional activity of the glioma-associated oncogene (GLI) [73]. Hh-Gli pathway has been shown to be critical in tumorogenesis [73–76], affecting the stabilization and guidance of cytoneme [77], and downregulating EMT [78–80] in crosstalk with Wnt [81], TGF-β [82], and P13K-AKT [83,84]. Furthermore, the orientation and guidance mechanisms followed by the Hh-Gli pathway have recently been studied [85], as well as the role of the Hh co-receptor interference hedgehog (Ihog) in contributing to integrin-mediated focal adhesions [86]. Therefore, this Hh-Gli pathway, which is responsible for regulating cell growth and renewal when it is regulated and for tumor growth when it is deregulated, strongly correlates with the aforementioned biochemical and mechanical processes.

To conclude, we summarized and unified examples of biological pathways currently being studied to open a perspective that connects mechanotransduction mechanisms with mathematical models. The structure of the ECM emerges as a critical therapeutic driver, as the stiffness of the ECM is closely related to a poor prognosis of the disease in the proposed pathways. Therefore, mechanotherapy should focus on modifying the biochemical and biomechanical properties of the tumor microenvironment and balance pathways that prevent tumor progression.

In particular, this work deals with the stress states of the tumor and their implications on carcinogenesis (Section 2) to later explain how to include mechanics in multiscale biomathematical models in the third section. First, we establish the framework on which the growth models and the mechanical interactions are based, and second, review the models proposed in the literature in the last decades to point out those studies that consider mechanotransduction in growth. Finally, we refer to Section 4 to sketch the main ideas that have emerged to tackle the tumor microenvironment that produces controlled mechanotransduction.

2. Mechanical stresses on tumors

As discussed in the previous section, the fate of tumors is highly influenced by mechanics. In addition to well-studied biochemical factors such as hypoxia and angiogenesis [87–92], mechanical forces play a critical role in tumor development. Tumors can be considered as a poroelastic medium composed of interstitial fluid and solid components (cells, extracellular matrix, filaments, nanotubules, and protrusions) that deform according to the stresses to which they are subjected, depending not only on the duration and direction of the forces, but also on the mechanical properties of the tumor and its environment [2,93,94]. The literature has used the term *pressure* in different contexts [95–99]. Some refer to internal tumor stresses that keep the homeostatic state of the tissue, to possible external stress applied to tumors, to the interstitial fluid pressure, to the mutual pressure exerted by two dynamic cell populations across their interface, and even to the fluxes of cells. Here, we refer to *pressure* as compression stress. We denote by stresses the

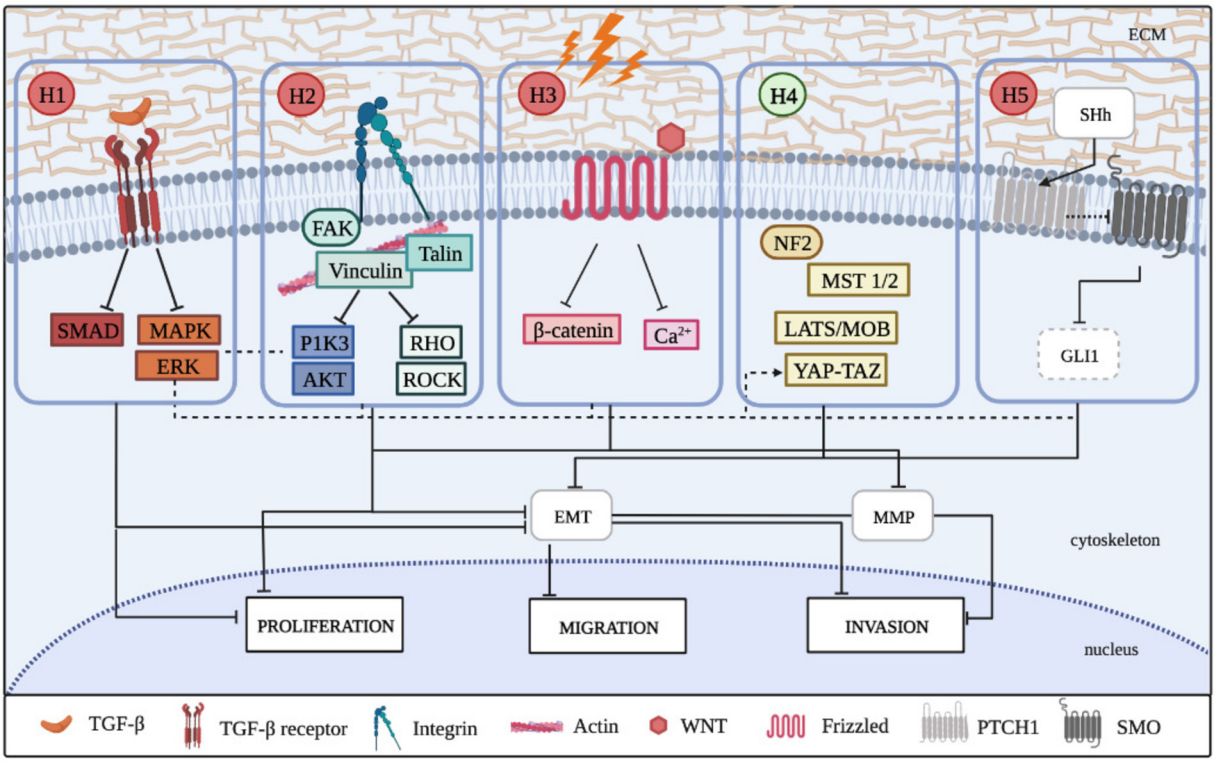

Fig. 1. Examples of the therapeutical targets to impact cancer cells via mechanotransduction. From left to right, the mechanisms proposed are H1) Inhibition of TGF-β in advanced stages of the disease, H2) Deregulation of Integrin-focal adhesions to prevent the activation of P13K-AKT and RHO-ROCK pathways and their associated malignancy behavior, H3) Knockdown of Wnt-Frizzled to hinder poor prognosis, H4) Keep Hippo-pathway regulation to inhibit the YAP-TAZ nuclear localization and H5) Block overexpression of Hedgehog to prevent the inactivation of PTCH1 or Ihog. Mechanotherapy should account for these or other target mechanisms to selective block tumor progressors and the pathways that upregulate cancer propagation. Complete proteomics analyses should test the therapeutic hypotheses in different tumor cells, stages, and stress states.

internal and external forces applied to different tumor surfaces, regardless of their solid or fluid nature. Finally, the flow of cells is called flux.

In this review, we consider the dependence of the total stress state of the tumor on solid stress and fluid stress (Fig. 2). Solid stress increases as a function of tumor volume gain and the internal interaction between cells, ECM, and cell components that cause elastic rearrangements. In particular, external forces also impact tumor behavior. Externally imposed static or dynamic compressive stresses on tumors cause proliferation inhibition and induce cell apoptosis. The first evidence of mechanical stress induction was confirmed in 1997 when Helmlinger et al. reported measurements of adenocarcinoma spheroids embedded in agarose gel matrices with different concentrations [100]. The results suggested that spheroid growth was completely inhibited at 1% gel concentration. However, [100] also demonstrated the reversible behavior of the inhibitory effect, which implies that cells remain in a quiescent state as long as stress does not cease. Further experiments carried out in successive years for different cancer cell lines supported the results of [100]. Roose et al. performed experiments for spheroids of the human melanoma cancer cell line (MU89) at concentrations of 0.5% and 1% of type VII agarose [95]; Cheng et al. embedded spheroids of metastatic murine breast carcinoma (EMT6) and non-metastatic murine mammary carcinoma (67NR) monolayer cells in agarose gel [101]; Montel et al. experimented with carcinoma cell spheroids (CT26) [102] and reference [103] used multicellular spheroids of HT29, CT26 and BC52 cells. All analyses reached the same conclusion: the growth reduction was the result of compressive stress. To quantify the relationship between the concentration of the agarose gel (% w/w of Dextran) and the pressure (Pascals) exerted by the gel, the studies of [102–104] adapted the empirical formula proposed by [105]. From stress quantification, it is inferred that the compression applied in the above experiments reached values between 5-10kPa, achieving at least a 50% reduction in proliferation compared to stress-free growth and a 30% increase in apoptotic cell activity.

These findings reveal that not only the surrounding medium can exert pressure on the tumor but also that any external or internal stress could affect the tumor dynamics. In particular, it has been shown that if compression is exerted externally by a piston with adjustable weights, the direction of stresses affects the final shape of the tumor as proliferation is inhibited in areas of high pressure, resulting in different patterns [101]. Furthermore, monolayer peripheral cells can undergo a phenotypic transformation that causes cells to become leader cells and initiate collective migration [106], although other studies prove that compressive stresses through low ultrasound slow migration [107]. Another method of compressing tumors is to seed the spheroids in permeable microcapsules. In fact, [108] found that the difference in stiffness affects not only growth but also the thicknesses of the matrix.

Some of these studies are reviewed in [109], where their findings are summarized according to the source of the stresses. The relevance of these findings lies in their potential to design new cancer therapies: How could we modify the tumor microenvironment and alter the fate of the tumor? The last section of this review proposes an answer to this question.

In addition to the external stresses, growth and reorganization, cell-cell and cell-ECM interactions, cause internal stresses within the tumor. The stresses generated during growth alter tumor patterning [101,110] as well as biochemical components and the delivery of drugs [111–114]. Compressive radial and circumferential stresses can be distinguished in the core of the tumor, while at the interface, stress is compressive in the radial and tensile in the circumferential direction [2,115,116]. The forces generated can be quantified by traction microscopy, micropillars, cantilevers, and other techniques such as laser ablation and force interference [99].

The interaction of cell components and their environment also causes different levels of stress within the tumor. The existing forces between cell bounds (cell-cell adhesion mediated by E-cadherin proteins) keep the tumor stable in a homeostatic state. Notwithstanding, if adjacent clusters of cells have significantly different mechanical parameters, E-cadherins could sense the stiffness of cells and activate pathways that regulate cell adhesion [97,117,118]. Thus, the stiffest cluster of cells will compress the softest, generating forces that may allow the progression of the pulled fronts and the displacement of the softest tissue [2,97,119]. Furthermore, a patch of cells with identical mechanical properties can mutate and grow faster or slower than its environment, i.e., not uniformly compared to the rest of the tissue [96, 98]. As cells adhere to each other, cell patches transmit and accumulate stresses in a feedback mechanism: non-uniform growth generates pressure, which self-regulates growth [98,99]. The underlying biological theory of these local mechanical interactions is based on the cytonemes (filopodia-like structure) that mediate the mechanosensing of cellular communication among the closest cells [77,120].

Cell-cell adhesions and matrix-cell adhesions also sense changes in extracellular matrix properties through some of the membrane receptor proteins discussed in Section 1. In particular, the strength and contractility of adhesions regulate durotaxis [121,122], explaining why adhesion forces are considerably more robust in metastatic cells compared to non-metastatic cells [123,124]. In fact, the mechanical state of cells depends on the stiffness and the amount of stored elastic energy [125–128]. Reference [125] showed that cells exhibit a stiffer cytoskeleton on a stretched substrate than cells seeded on an unstretched gel and that cells elongate with substrate reciprocity [122]. Regarding the stress state of the primary tumor, cells rearrange and modify their microenvironment, generating internal forces that interact with external forces. These solid stresses that accumulate in the tumor during growth conform the residual stress, which has been computationally and experimentally quantified by the tumor excision and opening [111,115,129–132].

From the fluid perspective, the primary fluid stresses that affect tumor dynamics are the interstitial fluid pressure of the tumor (IFP or TIF) and the capillaries pressure (blood vessels and lymphatic system) [114], which interact with the extracellular medium by perfusion. These movements of perfusion and flow generate mainly fluid shear stresses (FSS) within the tumor and prevent fluid accumulation in interstitial spaces under normal conditions [2].

Fluid shear stress is an essential regulator of tumor cell adhesion and extravasation [133], affecting fluid mechanics and metastatic potential, since tumor cells are primarily subjected to interstitial and blood shear stress during metastasis to target secondary organs [133,134]. Invading tumor cells can take advantage of interstitial flow to generate autologous chemokine gradients, guiding their migration toward draining lymphatic vessels. Simultaneously, cells in the microenvironment also respond to elevated interstitial flow caused by tumors, precipitating a cascade of changes in cell phenotype, secretion of pro-invasive cytokines, and matrix remodeling, all of which enhance tumor invasion [135]. However, there are other critical factors in extravasation and metastasis, such as the necessary cooperation of EMT cells that alter the surrounding matrix through MMP and non-EMT cells that establish colonies at secondary sites [136].

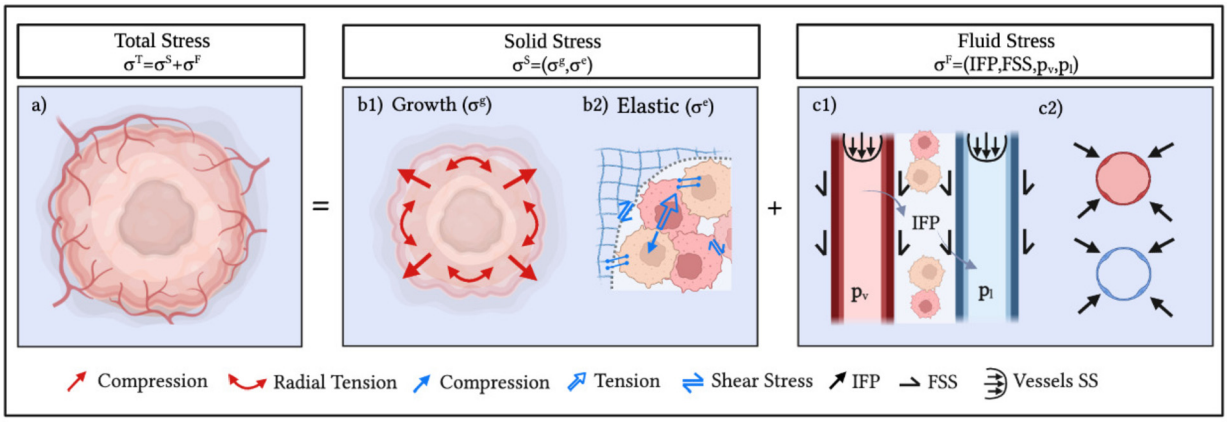

Fig. 2. Stress in a poroelastic tumor. a) Total stress is the sum of solid and fluid stresses generated during growth. b) Solid stress accounts for growth and elastic stresses. In particular, b1) shows the tensional growth state, which decomposes in radial compression and tension in the rims, while b2) accounts for the elastic rearrangement produced during growth: compression, shear, and tension forces that maintain equilibrium. Note that homeostasis is maintained if the cell-cell and cell-ECM adhesion forces are equilibrated. Finally, c1) fluid stresses are mainly shear and account for FSS in the interstitial medium and the shear stress of blood and lymphatic vessels. IFP arises with growth compressing the vessels (see the cross-section of vessels in subfigure c2).

Hyperpermeability of blood vessels and loss of lymphatic drainage within the tumor [137] represent barriers to drug delivery and transport [128]. As a result of that high vascular permeability, interstitial shear stress can reach approximately 0.01 Pa [133,138]. Blood shear stress levels are higher than those produced by interstitial and lymph flow, with pressure values in veins, capillaries, and arteries of 0.1-0.4 Pa, 1-2 Pa, and 0.4-3 Pa, respectively [133,139]. The lymphatic system drains and allows the re-entry of body fluid into the circulatory system, reaching an average pressure of 0.1 Pa [133], lower than the other FSS. The interstitial fluid pressure is isotropic and elevated due to total tumor stress [115], and it increases due to hyperpermeability of the blood vessels described above. The IFP is heterogeneous within the tumor: it rises at the core and decreases at the borders [115,140], and it becomes a modulator of tumor proliferation, enhancing duplication if the IFP is elevated [141]. In fact, the drainage of the interstitial fluid in a tumor xenograft model reversibly decreases tumor cell proliferation by improving drug uptake, modifying tumor patterning, and increasing the relaxation of the cortex [142].

Fluid forces can be measured by microfluidic traction force microscopy, confocal microscopy, and flow magnetic resonance imaging [133]. Furthermore, the classical Wick-in-needle (WN) and pressure catheter (PC) are the two most commonly used methods to measure fluid pressure directly [143], and magnetic resonance imaging (MRI) has been used to measure wall shear stress [144,145].

Thus, little changes at the microscale, like cell-cell and cell-ECM interactions, translate into changes at the macroscale through mechanotransduction pathways and vice-versa in dynamic reciprocity. In particular, solid stresses compress the vessels, causing a decrease in vascular perfusion [146], hindering homeostasis and the flow of nutrients to the solid tumor and increasing IFP while slowing lymphatic drainage. As a result, there may be a barrier to drug delivery, and tumor cells tend to increase the release of proangiogenic factors at the microscale, resulting in a highly impermeable drainage system that contributes to the malignant activity of the tumor cells [147].

To summarize, the tumor dynamic is involved in the accumulation of stress and the mechanical properties of the tumor and its environment, which in turn induces feedback into the biochemical pathways. Although the described solid and fluid effects are not mutually exclusive and a combined effect between stiffness and viscosity may coexist, in this review, we propose to classify tumor dynamics into two major groups according to the leading nature of their progression: solid and fluid behavior of tumors.

First, we distinguish the case in which the matrix, surrounding tissue, or external stresses hinder tumor growth or migration by exerting compressive stresses on tumor tissue (Fig. 3a). This case corresponds to the above experiments of agarose gels, where tumor development is slow if the tumor is embedded in a more rigid medium. In vivo, this fact is shown in prostate cancers, where benign prostatic hyperplasia exerts compressive stresses on the tumor and slows tumor progression [127,148,149].

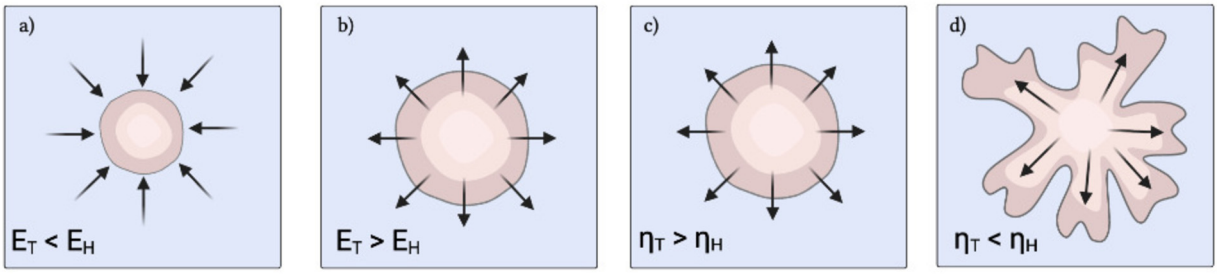

Fig. 3. Different patterns in tumor growth. The symbol E refers to the Young modulus, while η indicates viscosity. T and H subscripts refer to the tumor and healthy medium, respectively. a) and b) account for solid growth behavior, and c) and d) for fluid growth behavior. In particular, a) shows the inhibition of growth due to compressive solid stress, b) growth as solid mass effect, c) homogeneous tumor growth due to similar fluid properties, and d) the viscous fingering effect.

In the opposite case, it is the tumor – more rigid – that causes compressions in the environment, thus displacing the surrounding tissue in a process called the mass effect, in which it gains volume and grows (Fig. 3b). This phenomenon could explain why stiffer tumors can progress over the surrounding tissue [150], creating joint forces that will depend on both tissues' relative stiffness and accumulate throughout the growth process. Although tumor stiffness is characteristic of each cell line, average tumor stiffnesses range from 0.5-3kPa for spheroids [151] to 10-60kPa for consolidated tumors [152–154]. A suitable explanation of the difference between spheroids and consolidated tumors may rely on their function: cells and spheroids tend to be softer to adhere to each other, promoting motility, while consolidated tumors behave as a solid mass with strong links and fibers. To characterize the mechanical properties of tumors, some techniques such as static and dynamic nanoindentation, micropipette aspiration, and optical tweezers are used in vitro [151,155,156]. The last technology combines mechanical characterization of cells with incubation and imaging to provide in vivo-like conditions (Pavone by © Optic11). At the macroscale level, elastography is used [150,157,158].

However, the hypothesis that the growing tumor displaces the surrounding tissue or vice versa is debatable when the stiffness of the medium and the tumor are similar. Why can the tumor then migrate and proliferate? The latest studies propose a possible explanation based on the fluid behavior of tumors. Specifically, they are based on viscosity differences between the medium and the tumor [159–161]. This event has been well studied in fluids, where a fluid with a lower viscosity is injected into a fluid with a higher viscosity. The experiment develops Saffman-Taylor instabilities, commonly known as viscous fingering due to its pattern. In turn, instabilities do not occur if viscosities are reversed [159,162,163].

Finally, these processes show a new perspective on tumor dynamics: growth and migration may be caused by the viscosity difference rather than the difference in stiffness. Hence, the tumor grows homogeneously if the viscosity of the medium is higher than that of the tumor (Fig. 3c) in an analogous way to the case of the mass effect and heterogeneously if the tumor is less viscous than the medium, forming patterns characteristic of viscous fingering and more aggressive tumors (Fig. 3d).

Along these lines, recent reports show that glioblastoma (aggressive and metastatic tumor) is less viscous than healthy brain parenchyma [159,164], although in this case the fibrillar structure of the ECM (porosity, stiffness, etc.) as well as the protein distribution of the brain – which can act as attractor or repulser signals – have an additional influence on the directions of migration [85,165,166].

3. Biomechanical models of tumor growth

Mathematical biomechanical models emerged in the mid-1990s to consider the mechanisms of the microenvironment and the stresses generated in tissue growth. Tissues can be modeled using continuum mechanics since they can be understood as homogenized multiphasic materials. In the framework of tumor mechanics, some authors propose modeling tumors as discrete elements, considering the microenvironment surrounding them. The most commonly used discrete models are based on whether cells are on a structured mesh (on-lattice models) or not (off-lattice models), which, according to [167] are not realistic to represent the cell motion nor to consider fixed cell geometries, respec-

tively. For further reading, we recommend reference [168], which reviews some of these discrete models, including a list of open computational software to model them.

However, in this review, we describe the main approaches of the macroscale continuum from finite growth theory and its simplification into infinitesimal growth theory, which neglects the discontinuities on microscopic levels considering the tumor microenvironment as continuously distributed in the entire space it occupies. The fundamental theory that underpins the growth of tissues from mechanics emerges from the works of [130,169,170] and the subsequent review of the literature by [171]. Since then, studies have focused mainly on the theory of soft tissue growth and remodeling [172,173], without specific application to tumor modeling. However, some authors have specialized in cancer, considering growth with solid and fluid phases [95,115,128,131,174]. More recently, [115,128] summarized their comprehensive approach to tumor modeling from different angles: fluid and solid mechanical models, drug delivery, vascularization, and angiogenesis. The main equations of these models include multiphase systems, momentum balance, constitutive behavior, mass balance that account for net proliferation and motility, and diffusive laws for biochemical components.

Due to the significant increase in models developed within the last decade, in this section, we propose to unify and classify the biomechanical models of growth known to date. Although previous researchers have accounted for the solid and fluid phases of the tumor, as described in Section 2, there are still no models described, to our knowledge, that include viscosity differences - beyond mass and solid stress differences - able to predict fluid tumor propagation phenomena (i.e. viscous fingering).

3.1. Fundamentals of mechanics

To explain the growth of tumors from mechanics, we first introduce the basic concepts of Finite Strain theory [175] based on the Classical Continuum Mechanics (CCM). Let P be a point in the undeformed body B at the initial time t=0, and in the undeformed configuration k_o, which deforms to the point p in the deformed body b at time t in the current configuration k_t (Fig. 4). The point P is located at the material, or Lagrangian coordinates $\mathbf{X}$, and p is located at the spatial, or Eulerian coordinates $\mathbf{x}$. Thus, the initial position is represented by $\mathbf{X}$ while $\mathbf{x}$ denotes the position after a time t when the body is deformed. Particle displacement, referred to as a function of material coordinates, is expressed by Equation (1).

$$\mathbf{u}(\mathbf{X}, t) = \mathbf{x}(\mathbf{X}, t) - \mathbf{X}. \tag{1}$$

The material deformation at a material point is given by the gradient tensor $\mathbf{F}$, which relates the reference and current configuration by Equation (2).

$$\mathbf{F} = \frac{\partial \mathbf{x}}{\partial \mathbf{X}}. \tag{2}$$

Consider dV the volume occupied by a particle and $\rho_o(\boldsymbol{X})$ the density at the initial undeformed configuration $k_o(B)$. Thus, the mass of the particle is given by $dM_o = \rho_o dV$. After a time interval, dv and ρ are the volume and density at the current deformed configuration $k_t(b)$. The change in volume or density due to deformation is described by the determinant of the deformation gradient as J=|$\mathbf{F}$| or in terms of volume or density variation between the current and initial configuration $\mathrm{J} = \dfrac{dv}{dV} = \dfrac{\rho_o}{\rho}$. Then, the conservation of mass for a single constituent in Lagrangian and Eulerian coordinates is:

$$\begin{aligned} \rho_o(\mathbf{X}) &= \mathrm{J}(\mathbf{X}, t)\rho(\mathbf{X}, t), \\ \frac{\partial \rho}{\partial t} + \nabla \cdot (\rho \mathbf{v}) &= 0, \end{aligned} \tag{3}$$

where the velocity of the particle is given by $\mathbf{v} = \dfrac{\partial \mathbf{x}}{\partial t}$. The finite deformation of the Green-Lagrange symmetric tensor $\mathbf{E}$ is defined to account for the strains.

$$\mathbf{E} = \frac{1}{2} \cdot \left(\mathbf{F}^{\mathbf{T}} \mathbf{F} - \mathbf{I} \right), \tag{4}$$

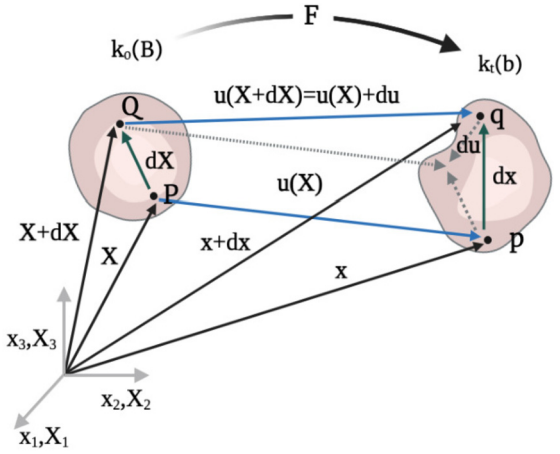

Fig. 4. Fundamentals of mechanics: Configurations, Displacements, and Deformations.

where **I** is the second-order identity tensor. Furthermore, the Green-Lagrange symmetric tensor **E** can be expressed in terms of displacements **u**, as:

$$\mathbf{E} = \frac{1}{2}\Big(\nabla \mathbf{u} + \nabla \mathbf{u}^{\mathrm{T}} + \nabla \mathbf{u}^{\mathrm{T}} \cdot \nabla \mathbf{u}\Big). \tag{5}$$

The strain energy density is the energy stored in the tissue during stretching, and the use of different strain energy functions W depends on the behavior of the tumor. Stresses are obtained by deriving the strain energy density with respect to **E** or strain deformation invariants, obtaining different constitutive equations. The invariants are tensors that satisfy the principle of material frame indifference and do not change with the Eulerian or material framework rotations. The invariants used in this review are mainly used in nonlinear elasticity, see equation (6). They are applied to a generic tensor **A**.

$$\begin{aligned} \mathrm{I_A} &= \mathrm{tr}(\mathbf{A}), \\ \mathrm{II_A} &= \frac{1}{2}\Big((\mathrm{tr}(\mathbf{A}))^2 - \mathrm{tr}(\mathbf{A}^2)\Big), \\ \mathrm{III_A} &= |\mathbf{A}|, \end{aligned} \tag{6}$$

Regarding stresses, it is common to use the second Piola-Kirchoff pseudo-stress tensor **S**:

$$\mathbf{S} = \frac{\partial \mathrm{W}}{\partial \mathbf{E}} = \frac{\partial \mathrm{W}}{\partial \mathrm{I_E}}\frac{\partial \mathrm{I_E}}{\partial \mathbf{E}} + \frac{\partial \mathrm{W}}{\partial \mathrm{II_E}}\frac{\partial \mathrm{II_E}}{\partial \mathbf{E}} + \frac{\partial \mathrm{W}}{\partial \mathrm{III_E}}\frac{\partial \mathrm{III_E}}{\partial \mathbf{E}}, \tag{7}$$

where the invariants refer here to the finite Green-Lagrange deformation tensor. However, other stresses are commonly used for convenience of configuration. In the Lagrangian approach, the first Piola-Kirchoff stress tensor **P**, which associates the undeformed body to the stresses at the current configuration. In the Eulerian formulation, the Cauchy stress tensor –real stress– $\boldsymbol{\sigma}$ is referred to as the deformed body b in the current configuration. The relation between pseudo-stresses and the Cauchy stress tensor is given by Equation (8).

$$\begin{aligned} \mathbf{P} &= \mathrm{J}\boldsymbol{\sigma}\mathbf{F}^{-\mathbf{T}}, \\ \mathbf{S} &= \mathrm{J}\mathbf{F}^{-\mathbf{1}}\boldsymbol{\sigma}\mathbf{F}^{-\mathbf{T}}. \end{aligned} \tag{8}$$

Another widely used notation is that described by the Cauchy-Green deformation tensors: the right Cauchy-Green deformation tensor $\mathbf{C} = \mathbf{F}^{\mathbf{T}}\mathbf{F}$, and the left Cauchy-Green deformation tensor $\mathbf{B} = \mathbf{F}\mathbf{F}^{\mathbf{T}}$. Considering the deformation tensor and the relation among pseudo-stresses, other formulas that can be found in the literature are:

$$\begin{aligned} \mathbf{P} = \mathbf{F}\mathbf{S} &= \frac{\partial \mathrm{W}}{\partial \mathbf{F}} = \mathbf{F}\frac{\partial \mathrm{W}}{\partial \mathbf{E}} = 2\mathbf{F}\frac{\partial \mathrm{W}}{\partial \mathbf{C}}, \\ \mathbf{S} = \mathbf{F}^{-\mathbf{1}}\mathbf{P} = \mathbf{F}^{-\mathbf{1}}\frac{\partial \mathrm{W}}{\partial \mathbf{F}} &= \frac{\partial \mathrm{W}}{\partial \mathbf{E}} = 2\frac{\partial \mathrm{W}}{\partial \mathbf{C}}. \end{aligned} \tag{9}$$

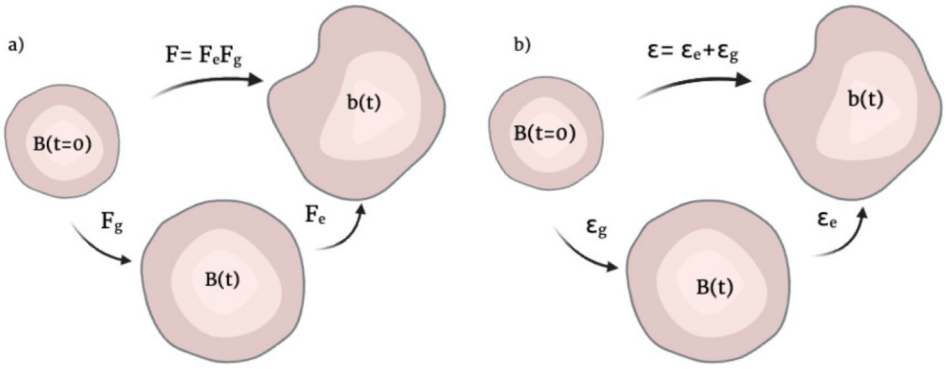

Fig. 5. Fundamentals of growth theory. a) Finite growth theory. b) Infinitesimal growth theory.

Last, the equilibrium of the system is achieved if the balance momentum is guaranteed:

$$\nabla \cdot \mathbf{P} + \mathbf{b} = \rho_o \frac{\partial^2 \mathbf{u}}{\partial t^2}, \tag{10}$$

where $\mathbf{P}$ depends on the constitutive material behavior of each tissue, ρ_o is the material density, $\mathbf{b}$ are the body forces, and the term on the right accounts for the inertia terms. Note that the characteristic velocities in biological tissues and growth are small, so inertia terms are usually neglected.

3.2. Tumor growth from mechanics

Once the mechanical basics are set, tumor growth is included in the mechanics' framework similar to the thermoelastic problem [175,176]. Then, the expansion or resorption of the tumor causes deformation, and there is a subsequent elastic rearrangement to ensure the equilibrium of the medium. According to that, the deformation gradient tensor decomposes multiplicatively into the growth tensor $\mathbf{F_g}$ and the elastic tensor $\mathbf{F_e}$ (Fig. 5a), although a third component could also be included to account for residual stresses accumulated in tumors [104,115,130,177].

$$\mathbf{F} = \mathbf{F_e F_g}, \tag{11}$$

where $\mathbf{F}$ is the total deformation gradients, $\mathbf{F_e}$ is the elastic rearrangement produced after tumor dynamics and $\mathbf{F_g}$ considers the gain or resorption of tumor mass described by the stretch rate g, $\mathbf{F_g} = g\boldsymbol{\lambda_g}$, with $\boldsymbol{\lambda_g}$ the anisotropy tensor that distributes growth in different directions through different weights. If the growth tensor is taken as isotropic, then $\boldsymbol{\lambda_g} = \mathbf{I}$.

Just as it happened with the Jacobians of deformation, the changes in volume or density produced by growth are described by the determinant of the deformation gradient $J_g = |\mathbf{F_g}|$. Then, if $J_g > 1$ growth takes place while if $J_g < 1$, resorption occurs. The mass conservation that now accounts for mass gain or resorption can be expressed in a Lagrangian or Eulerian frame reference:

$$\begin{aligned} \frac{d(\rho J)}{dt} &= J\rho\Gamma, \\ \frac{\partial \rho}{\partial t} + \nabla \cdot (\rho \boldsymbol{v}) &= \rho\Gamma, \end{aligned} \tag{12}$$

where the source term Γ accounts for the gain or loss of tumor mass. Some describe growth as an increase in the mass of already existing particles (cells) in the body [172,178] while others account for the increase in the particles – proliferation or duplication of cells – and its motion – motility or migration–. Thus, Γ is usually expressed as a net proliferation and has been formulated by some phenomenological laws such as exponential, Gompertzian, logistic and even stochastic equations to account for the large variability of the experiments [119,179]. Furthermore, growth dynamics can also be a function of the availability and concentration of nutrients [95,131,172], the generation or degradation of some cellular components [177,180,181], proteins [127,165], drugs [131,182] and stress [183] as it is

pointed out in the next section. The relationship between the term of the isotropic growth strain and the proliferation rate is given by [172]:

$$\frac{dg}{dt} = \frac{1}{3} g\Gamma. \tag{13}$$

Furthermore, volumetric fractions are used to model the multiphase tumor system. Considering that the cell density of each phase is $\rho_i = \frac{\partial m_i}{\partial v}$, the volumetric fraction occupied by a phase can be represented by $\phi_i = \frac{\partial v_i}{\partial v}$. The classical theory of the growth of mixtures implies that the mass densities of each phase can change, but only in such a way that the mass is conserved [172,184], which means that there can be a mass exchange, but not real mass production [185, 186]. This overcomes the limitation of the theory of growth, in which there is a violation of the Continuum principle by creating new points [176]. The existence of different phases can be expressed as:

$$\phi_F + \sum_{i=1}^{n} \phi_i = 1, \tag{14}$$

where the subindex F refers to the interstitial fluid and the subindex i denotes the constituents of the solid tumor. However, some authors support the creation of mass during tumor growth, so the previous equation is no longer satisfied, and the sum of the constituents would exceed the unit [187,188]. Finally, it is usual to find mass continuity in volumetric fractions. Specifically, the mass conservation of the fluid and solid phases is a function of time and space:

$$\begin{aligned} \frac{\partial \phi_F}{\partial t} + \nabla \cdot (\phi_F \, \mathbf{v}_F) &= \phi_F \Gamma_F; \\ \frac{\partial \phi_i}{\partial t} + \nabla \cdot (\phi_i \mathbf{v}_i) &= \phi_i \Gamma_i. \end{aligned} \tag{15}$$

In addition to cell proliferation Γ_i, multiphase systems can involve feedback and interactions between different solid phases. This phenomenon is known in modeling as predator-prey dynamics or Volterra–Lokta equations [187, 189]. Lastly, the motility of the various solid phases includes the use of a flux term $\boldsymbol{\mathcal{J}}_i$:

$$\frac{\partial \phi_i}{\partial t} + \nabla \cdot (\phi_i \mathbf{v}_i) = \nabla \cdot \left(\upsilon \boldsymbol{\mathcal{J}}_i \right) + \phi_i \Gamma_i, \tag{16}$$

where υ is the diffusion-type coefficient. Flux $\boldsymbol{\mathcal{J}}_i$ is usually defined as linear and isotropic, even though its linearity hinders the regulation of the propagation front, which is inherent to each cell species [190]. To overcome this drawback, some studies suggest adding a relaxation term that limits the infinite propagation speed characteristic of linear diffusion using relaxation terms [191]. Others define a finite-speed tumor propagation front through the porous medium equation (PME): $\boldsymbol{\mathcal{J}}_i = \phi_i \nabla j_i$, with $j_i = \phi_i^m$ and $m \geq 1$ [192], and its limitation through second-order terms by Brinkman's law [193,194]. References [96,165,195–199] use a flux-saturated PME with measurable propagation speed c_i, defining the flux of cells as:

$$\boldsymbol{\mathcal{J}}_i = \left(\frac{\phi_i}{\sqrt{\phi_i^2 + \left(\frac{\upsilon_i}{c_i} \right)^2 |\nabla \phi_i|^2}} \nabla \phi_i^m \right). \tag{17}$$

Regarding the different phases that make up the continuum, equation (11) should be described for each phase as $\mathbf{F}_i = \mathbf{F}_{\mathbf{e}i} \mathbf{F}_{\mathbf{g}_i}$.

3.2.1. Simplification into infinitesimal growth theory

The continuum can be modeled by considering infinitesimal theory, assuming that the displacements and rotations of the tumor are small enough compared to the initial size of the tumor. Notwithstanding, the selection of the strain theory is thus dependent on the purpose of the study. To move from the multiplicative decomposition of large strains to the additive decomposition of small strains (Fig. 5b), we define the polar decomposition of the gradient tensor $\mathbf{F}$:

$$\mathbf{F} = \mathbf{RU}, \tag{18}$$

with $\mathbf{U}$ the right stretch tensor and $\mathbf{R}$ the rotation tensor. In particular, the stretch tensor is defined by:

$$\mathbf{U} = \sqrt{\mathbf{F}^{\mathbf{T}}\mathbf{F}} \approx \mathbf{I} + \boldsymbol{\varepsilon} + h.o.t., \tag{19}$$

where the small strain tensor is defined by $\boldsymbol{\varepsilon} = \frac{1}{2}\left(\nabla\mathbf{u} + \nabla\mathbf{u}^{\boldsymbol{T}}\right)$ and $h.o.t.$ refers to high-order terms.

The rotation tensor is:

$$\mathbf{R} = exp(\boldsymbol{\Theta}) \approx \mathbf{I} + \mathbf{e}\boldsymbol{\Theta} + h.o.t., \tag{20}$$

with $\mathbf{e}$ is the Levi-Civita tensor and $\boldsymbol{\Theta}$ the rotation tensor. Combining equations (18), (19) and (20), and assuming $\boldsymbol{\Theta} \ll 1$, then:

$$\mathbf{F} = (\mathbf{I} + \boldsymbol{\varepsilon})(\mathbf{I}) = (\mathbf{I} + \boldsymbol{\varepsilon}) + h.o.t. \tag{21}$$

Notice that the spatial derivative of displacements in equation (1) can be described as:

$$\frac{\partial \mathbf{u}}{\partial \mathbf{X}} = \frac{\partial \mathbf{x}}{\partial \mathbf{X}} - \mathbf{I} = \mathbf{F} - \mathbf{I} \longrightarrow \boldsymbol{\varepsilon} \approx \frac{\partial \mathbf{u}}{\partial \mathbf{X}} = \mathbf{F} - \mathbf{I}. \tag{22}$$

Using (21), assuming small strains and rotations, the multiplicative decomposition of (11) reads:

$$\mathbf{F} = \mathbf{F_e}\mathbf{F_g} = (\mathbf{I} + \boldsymbol{\varepsilon_e})(\mathbf{I} + \boldsymbol{\varepsilon_g}) = \mathbf{I} + \boldsymbol{\varepsilon_g} + \boldsymbol{\varepsilon_e}. \tag{23}$$

Finally, the infinitesimal growth theory is based on:

$$\boldsymbol{\varepsilon_e} + \boldsymbol{\varepsilon_g} + \mathbf{I} = \boldsymbol{\varepsilon} + \mathbf{I} = \mathbf{F}. \tag{24}$$

Then, Equation (11) simplifies into the additive equation (25):

$$\boldsymbol{\varepsilon} = \boldsymbol{\varepsilon_e} + \boldsymbol{\varepsilon_g}, \tag{25}$$

where $\boldsymbol{\varepsilon_e} = \frac{1}{2}(\nabla\mathbf{u} + \nabla\mathbf{u}^{\mathrm{T}})$ is the elastic small deformation that guarantees mechanical equilibrium and the volumetric growth deformation is $\boldsymbol{\varepsilon_g} = g\boldsymbol{\lambda_g}$. Considering small strains, the elastic Cauchy stress tensor may be expressed as:

$$\boldsymbol{\sigma_e} = \boldsymbol{\sigma} - \boldsymbol{\sigma_g}, \tag{26}$$

where $\boldsymbol{\sigma}$ is the total tensional state obtained from equation (7) and $\boldsymbol{\sigma_g}$ is the induced growth stress. Assume volumetric growth of the tumor, $\boldsymbol{\sigma_g} = \kappa\boldsymbol{\varepsilon_g}$, with κ the bulk modulus. Finally, note that the advective term of the mass continuity equation (16) would be negligible under the assumption of small displacements.

3.2.2. Constitutive behavior of tumors

Tumors are mostly considered hyperelastic and anisotropic materials, spatially and temporally heterogeneous, and their dynamic is strongly related to their mechanical properties. Due to the heterogeneous nature of the tumor, it is important to model the tumor's fluid component and the different elastic structures. For this purpose, the mixture theory is used [184,185]. We denote by $\mathrm{W_e}$ the strain energy density of the solid skeleton and by $\mathrm{W_p}$ the contribution of saturated pores to the strain energy density. The total contribution reads $\mathrm{W} = \mathrm{W_e} + \mathrm{W_p}$. Most of the constitutive relations of solid elastic used in the literature are the Blatz-Ko, Neo-Hookean, Exponential, and Ciarlet equations, as shown in Table 1. Although viscosity is a fundamental parameter in reorganization at small scales, viscosity is no longer relevant over long times – intrinsic to growth. Therefore, the equations of tumor behavior do not include the solid viscosity of the cells that could be described by the Kelvin-Voigt, Maxwell, or Burgers models. However, viscosity can be a crucial parameter in fluid behavior, as outlined in Section 2. Despite the different constitutive relations proposed, [177] concluded that the exponential law fits best the breast and colon adenocarcinoma experiments. However, the evolution of stress appeared to be independent of the chosen constitutive relation [177].

Considering the Biot theory of a porous material [205], the fluid strain energy can be modeled by a quadratic potential $\mathrm{W_p} = -\frac{\alpha}{2}(p - p_o)^2$. The variation of fluid content ζ assuming constant density is related to elastic volumetric strain, which depends on growth ε_v, and pore pressure p:

Table 1
Essential strain energy functions used in tumor growth modeling. λ, and μ are the first Lamé parameter, and the shear modulus, respectively. The invariants described above are related to the right Cauchy tensor (C) and the left Cauchy tensor (B). J_e is the elastic determinant and f, z, A_1, A_2 and C are constants.

Behavioral elastic relation	Main equation	Source
Comp. Neo-Hookean	$W_e = 0.5\mu(I_C - 3 + 2\ln J_e) + 0.5\lambda(J_e - 1)^2$	[177,181]
Comp. Blatz-Ko	$W_e = \frac{\mu f}{2}\left[(I_C - 3) - \frac{2}{z}(III_C{}^{z/2} - 1)\right] + \frac{\mu(1-f)}{2}\left[\frac{II_C}{III_C} - 3 - \frac{2}{z}(III_C{}^{-z/2} - 1)\right]$	[172,177,200]
Comp. Ciarlet	$W_e = \frac{\lambda}{4}\cdot(III_B - \ln III_B - 1) + \frac{\mu}{2}\cdot(I_B - \ln III_B - 3)$	[116,201,202]
Exponential	$W_e = A_1\left(\exp(C_1(-3 + I_C J_e^{-2/3})) - 1\right) + A_2(-1 + J_e)^2$	[177]
Comp. Linear	$W_e = 0.5\lambda(I_E)^2 + \mu I_E^2$	[96,127,203,204]

$$\zeta = \phi_F - \phi_{F0} = \frac{1}{M}(p - p_0) + \alpha\varepsilon_v, \tag{27}$$

where ϕ_F is the current fluid phase, ϕ_{F0} is the initial fluid content, α is the Biot coefficient, which represents the volume of fluid gained or lost when the pore pressure returns to its initial state [206], and M is the Biot modulus, which considers the increase in fluid amount as a result of a unit increase in the pore pressure, under constant volumetric strain [206,207]. Then, the fluid mass conservation can be rewritten as the well-known storage equation:

$$\frac{\partial\zeta}{\partial t} = \nabla\cdot\boldsymbol{q} + \Gamma_F \longrightarrow \frac{1}{M}\frac{\partial p}{\partial t} + \alpha\frac{\partial\varepsilon_v}{\partial t} = \nabla\cdot\boldsymbol{q} + \Gamma_F, \tag{28}$$

where the flux is represented by $\boldsymbol{q}$, and Darcy's law usually defines it, $\boldsymbol{q} = k\nabla p$, with k denoting the conductivity, which is a function of the dynamic fluid viscosity, the porosity, and permeability of the medium [205,206]. The term Γ^F considers fluid exchange between the lymphatic and vessel systems and interstitial fluid described in Section 2. Starling's theory can describe the flow rate:

$$\Gamma_F = k_v\Big[(p_v - p) - \omega(\pi_v - \pi_l)\Big] - k_l(p - p_l), \tag{29}$$

where p_v is the pressure of the blood vessel, ω is the reflection coefficient that weights the interstitial osmotic pressure $(\pi_v - \pi_l)$, and p_l is the drainage of lymphatic pressure that works in the opposite direction of the blood vessel system. The parameters k_v and k_l are the conductivity coefficients of the vessel and lymphatic system, which consider the velocity of fluid transfer through the capillary surfaces [137,208,209]. Interestingly, some authors proposed to model the conductivity of the lymphatic system as a linear function of the density of tumor cells, since tumor growth has been shown to increase IFP, decreasing lymphatic vessel drainage [189,210].

In addition to the intrinsic mechanics of growth, it is crucial to account for the multiscale dimension of the problem. Thus, some authors have also considered the microscale of biochemical interactions using reaction or reaction-diffusion equations, as described in (16). From these equations, they establish the dependence of growth on local oxygen [95,182,211], nutrients [200,212], proteins [127,165,213] and even the effect of therapy such as drug delivery [131,182]. In particular, slight variations of these substances prolonged in time can produce the same effect as a large instantaneous fluctuation. For instance, reference [77] shows that hypoxia processes and small (apparently negligible) Hh flow over time significantly influence growth or migration.

3.3. Modeling mechanotransduction in tumor growth

Tumor growth directly affects the stress state of the tissue. However, as demonstrated experimentally (see Section 2), stress is an important regulator of mechanotransduction directly involved in proliferation and migration. Hence, the growth laws must also account for the dependence of cellular and tissue stress on continuous feedback.

The first biomechanical models that involve mechanotransduction were proposed in [95], which formulated and validated a linear poroelastic model that accounts for the inhibition of proliferation of the melanoma tumor spheroid line (MU89) embedded in agarose gel matrices. Since then, mechanotransduction $\mathcal{M}$ has been modeled as a phenomenological function that affects migration and proliferation rates by stress.

Table 2
Mechanotransduction laws used in recent years. The parameters β_i, q, and χ_σ are related to the fitting of cell size and proliferation to relieve stress. The hydrostatic stress that accounts for volumetric changes is $\sigma_h = 1/3\,\mathrm{tr}(\boldsymbol{\sigma})$, Σ refers to the adhesion forces of the cells, and the Von Mises stress, which is a measure of the distortion energy, is defined by $\sigma_{vm} = \sqrt{\frac{(\sigma_1-\sigma_2)^2+(\sigma_2-\sigma_3)^2+(\sigma_3-\sigma_1)^2}{2}}$, where σ_i refers to main stresses. The stress threshold that cells sense is defined by σ_L, and it is characteristic of each cell line. The choice of what type of stress is considered depends on the purpose of the study, so other proposals such as Tresca stress could be included if the main source of mechanotransduction is shear stress.

Affected term	Mechanotransduction law	Source
Growth	$\mathcal{M} = 1 - \beta\sigma_h$	[95,137,177,180,182,187]
Growth	$\mathcal{M} = (1 - (\beta_1\sigma_h/\beta_2 + \sigma_h))$	[211]
Growth	$\mathcal{M} = \left[q + \frac{(1-q)exp(\chi_\sigma(\sigma_h-\sigma_L))}{1+exp(\chi_\sigma(\sigma_h-\sigma_L)}\right]$	[187,188]
Growth	$\mathcal{M} = 1 - \beta_1 \frac{\Sigma}{\Sigma+\beta_2}$	[104]
Migration	$\mathcal{M} = exp(-\beta\sigma_{vm})$	[190,214,215]
Migration and Growth	$\mathcal{M} = exp(-\beta_1(\sigma_{vm} + \beta_2\lvert\sigma_h\rvert))$	[127]

The key idea is that the forces present in the tumor are pressure-like and directly proportional to tumor cells through a function that describes the dependence of growth on solid stress. Taking into account the previous Eulerian equation of mass continuity described in (16), mechanotransduction is usually included in mass continuity as follows:

$$\frac{\partial\phi_i}{\partial t} + \nabla\cdot(\phi_i v_i) = \nabla\cdot(\mathcal{M}\upsilon\boldsymbol{\mathcal{J}}_i) + \mathcal{M}\phi_i\Gamma_i, \tag{30}$$

being $\mathcal{M}$ the mechanotransduction function that can affect migration (first term on the right) and proliferation (second term on the right). Table 2 shows the main mechanotransduction functions used in the literature to date.

Specifically, the contribution of modeling mechanotransduction translates into different approaches which fit experimental data described in Section 2. Some computational studies found that growth-induced stress promotes higher levels of solid stress in the tumor interior and lower in the periphery [137]. Furthermore, high compressive solid stress can collapse blood vessels in the tumor interior [137], negatively affecting drug delivery [180]. However, a highly vascularized region on the periphery of the tumor is associated with better oxygenation and positive drug delivery, such as chemotherapy [182] and nanomedicine [180].

Furthermore, [211] proved that stiffer cells propagate through softer tissue and [177] quantified 1.5 the number of times the tumor must be more rigid than its surrounding to displace it. [177] also suggests that solid stress involves tumor inhibition independently of the constitutive equation chosen, although it strongly depends on mechanical interactions with the surrounding host tissue. References [187,188] showed the interspecific competition of species that defines the Volterra-Lotka equations that describe the growth of tumor and healthy cells. Indeed tumor cells are inhibited if stress exceeds a critical threshold value.

Some studies also propose a pseudopotential stress law based on cell interaction's repulsive and attractive forces. In particular, [184] developed a switch function in which mechanotransduction occurs if there is compression on the membrane of proliferative cells. The works of [216,217] change the law for a monotonic mollifier of the step function, and more recently [104] propose four mechanotransduction functions (linear, exponential, inversely proportional, and Michaelis-Menten-like equation – shown in Table 2) fitting experiments.

Considering also the effect of mechanotransduction on migration, [214] reconstructed the coupling parameter β from Magnetic Resonance Imaging (MRI). This could be one of the critical points in personalized mechanotransduction models, including chemotherapy effects. More recently, the intra-tumoral heterogeneity of gliomas [190] and the impact of drug delivery in breast tumors were also included in the mechanically coupled equations [215]. Lastly, [127] proposed a personalized prostate cancer model in which not only stress-driven growth, but also the mechanics produced by benign hyperplasia slow tumor growth. This is the only function of mechanotransduction known, as far as we are aware, that accounts for migration and proliferation terms and for both Hydrostatic and Von-Misses stress.

These studies open a pioneering approach to cancer prognosis, where the potential of personalized treatments at different scales is based on critical biochemical-mechanical interactions.

4. Conclusions and perspectives

The importance of translating mechanotransduction into therapy is becoming increasingly clear. Hence, the following steps should focus on identifying mechanisms that alter and normalize the tumor microenvironment and mathematical models that allow modulation of these mechanisms and their mechanoresponses.

With that in mind, recent research has focused on selectively killing cancer cells through mechanotherapy. The use of low-intensity ultrasound (LIUS) and low-intensity pulsed ultrasound (LIPUS) has been shown to decrease cancer cell proliferation in at least 30-50% while healthy cells remained unaltered [50,218–225]. Moreover, some studies notice ultrasound inhibition of the collective spread of cancer cells in processes induced by wound healing [107,221].

Since cells are highly susceptible to shear stress, shear waves (SW) also emerge as a promising target therapy [226–228]. SW operate at lower frequencies than ultrasound, allowing mechanotransduction while minimizing the possible cytodisruption and cell resonance caused by ultrasound at high frequencies [229,230]. Furthermore, SW intensities would avoid indiscriminate ablation of cells produced by high-intensity focus ultrasound (HIFU). Regarding another oscillatory shear stress, the use of shear stress through pulses of perfused interstitial fluid can be observed [231].

Then, using mechanical waves (pressure or shear waves) is a promising technique that opens a line in therapy, since they can be remotely focused and have no collateral effects. Notwithstanding, further studies are necessary to determine the optimum use of frequency, amplitude, and duty cycles.

Other perspectives propose using drugs to modify the elasticity of the tumor microenvironment. The study conducted by [232] shows the effectiveness of a drug-loaded hydrogel matrix, which selectively captures and destroys cancer cells, attracting them to an optimized ECM stiffened at 20 KPa. Thus, the ECM acts as a stiffness filter, differentiating the tumor and healthy cells independently of the drug load applied [232]. More microenvironment alterations normalize the tumor matrix by degrading its collagen with bacterial collagenase treatment [233], or modifying the tumor microenvironment with pirfenidone [234], with the objective of alleviating solid stress and reducing IFP. The result is an improved vascular system (relief of compressions in the vascular networks), which facilitates the supply of other drugs to the tumor. Furthermore, the use of these drugs can be remotely regulated by magnetic nanoparticles (MNP) [235,236] and mechanical waves [237–239].

These findings evidence the potential effects of mechanotherapy that can be combined with other existing treatments to enhance their benefits. Furthermore, mechanotherapy also applies to other pathologies such as bone [240,241] and Parkinson's disease [242]. Then future research lines should focus on the mechanics that induce cellular mechanosponse.

Along with these new empirical advances, it is also essential to develop multiscale mathematical models that incorporate the effect of mechanotherapies such as LIUS. In addition to the critical threshold stress and the fitting parameters described in Table 2 and generally referred to here as $\boldsymbol{\sigma}_L$ and q, the mechanotransduction laws should now consider perceived stress as both static growth-induced stress $\boldsymbol{\sigma_s}$ – generated on the time macroscale, t – and dynamic ultrasound-induced stress $\boldsymbol{\sigma_u}$ – developed on the microsecond-second time scale, t_u –. Finally, as reported in Section 1, mechanotherapy is strongly dependent on protein pathways A and structure of the ECM, S. Then the mechanotransduction caused by LIUS should be modeled as follows:

$$\mathcal{M} = f(\boldsymbol{\sigma}_L, q, \boldsymbol{\sigma}_s, \boldsymbol{\sigma}_u, A, S). \tag{31}$$

To conclude, the preceding in this review highlights the potential and importance of mechanotherapy for tackling cancer at the experimental and computational levels, which requires joint modeling and medical engineering. In this context, mechanotherapy can improve cancer treatment, opening a pioneering and non-invasive way to treat tumor cells and an innovative and powerful approach that could help with the prognosis and design of personalized treatments. Thus, the new challenges of the coming years will provide answers to the still open questions: What configuration of mechanical parameters is necessary to inhibit tumorigenesis? What is the right combination of treatments for each patient? How can we anticipate disease progression and predict the possible effects of therapies?

Declaration of competing interest

The authors declare the following financial interests/personal relationships which may be considered as potential competing interests: Juan Soler reports financial support was provided by University of Granada. Juan Soler reports a relationship with Spanish Scientific Research Council that includes: funding grants.

Acknowledgements

This paper has been partially supported by the MINECO-FEDER (Spain) research grant number EQC2018-004508-P, PID2019-106947RA-C22 (B.B., J.M., G.R.) and RTI2018-098850-B-I00 (J.S.). This study was also funded by Ministry of Science, Innovation and Universities of Spain, project numbers PID2020-115372RB-I00 (B.B., G.R.), Consejería de Innovación, Ciencia y Empresa, Junta de Andalucía P18-RT-1653 (B.B., J.M., G.R.), PY18-RT-2422 & B-FQM-580-UGR20 (J.S.), and by Consejería de Universidad, Investigación e Innovación from Junta de Andalucía, P21.00182 (B.B., J.M., G.R.). Lastly, B.B. research was granted by the Ministry of Science, Innovation and Universities of Spain, FPU2017/01415. Funding for open access charge: Universidad de Granada / CBUA. Figures were created with Biorender.com.

References

[1] Yang C-M, Chien C-S, Yao C-C, Hsiao L-D, Huang Y-C, Wu CB. Mechanical strain induces collagenase-3 (MMP-13) expression in MC3T3-E1 osteoblastic cells. J Biol Chem 2004;279(21):22158–65. https://doi.org/10.1074/jbc.M401343200.

[2] Northcott JM, Dean IS, Mouw JK, Weaver VM. Feeling stress: the mechanics of cancer progression and aggression. Front Cell Dev Biol 2018;6:17. https://doi.org/10.3389/fcell.2018.00017.

[3] Broders-Bondon F, Ho-Bouldoires THN, Fernandez-Sanchez M-E, Farge E. Mechanotransduction in tumor progression: the dark side of the force. J Cell Biol 2018;217(5):1571–87. https://doi.org/10.1083/jcb.201701039.

[4] Huang W, Hu H, Zhang Q, Wu X, Wei F, Yang F, et al. Regulatory networks in mechanotransduction reveal key genes in promoting cancer cell stemness and proliferation. Oncogene 2019;38(42):6818–34. https://doi.org/10.1038/s41388-019-0925-0.

[5] Han B, Bai X-H, Lodyga M, Xu J, Yang BB, Keshavjee S, et al. Conversion of mechanical force into biochem.ical signaling. J Biol Chem 2004;279(52):54793–801. https://doi.org/10.1074/jbc.m406880200.

[6] Northey JJ, Przybyla L, Weaver VM. Tissue force programs cell fate and tumor aggression. Cancer Discov 2017;7(11):1224–37. https://doi.org/10.1158/2159-8290.CD-16-0733.

[7] Hoffman BD, Grashoff C, Schwartz MA. Dynamic molecular processes mediate cellular mechanotransduction. Nat 2011;475(7356):316–23. https://doi.org/10.1038/Nat.10316.

[8] Na S, Collin O, Chowdhury F, Tay B, Ouyang M, Wang Y, et al. Rapid signal transduction in living cells is a unique feature of mechanotransduction. Proc Natl Acad Sci 2008;105(18):6626–31. https://doi.org/10.1073/pnas.0711704105.

[9] Schwartz MA, DeSimone DW. Cell adhesion receptors in mechanotransduction. Curr Opin Cell Biol 2008;20(5):551–6. https://doi.org/10.1016/j.ceb.2008.05.005.

[10] Chin L, Xia Y, Discher DE, Janmey PA. Mechanotransduction in cancer. Curr Opin Chem Eng 2016;11:77–84. https://doi.org/10.1016/j.coche.2016.01.011.

[11] Vogel V. Mechanotransduction involving multimodular proteins: converting force into biochemical signals. Annu Rev Biophys Biomol Struct 2006;35:459–88. https://doi.org/10.1146/Annu.Rev.biophys.35.040405.102013.

[12] Hieda M. Signal transduction across the nuclear envelope: role of the linc complex in bidirectional signaling. Cells 2019;8(2):124. https://doi.org/10.3390/cells8020124.

[13] Martino F, Perestrelo AR, Vinarskỳ V, Pagliari S, Forte G. Cellular mechanotransduction: from tension to function. Front Physiol 2018;9:824. https://doi.org/10.3389/fphys.2018.00824.

[14] Geiger B, Spatz JP, Bershadsky AD. Environmental sensing through focal adhesions. Nat Rev Mol Cell Biol 2009;10(1):21–33. https://doi.org/10.1038/nrm2593.

[15] Jahed Z, Shams H, Mehrbod M, Mofrad MR. Mechanotransduction pathways linking the extracellular matrix to the nucleus. Int Rev Cell Mol Biol 2014;310:171–220. https://doi.org/10.1016/b978-0-12-800180-6.00005-0. Elsevier.

[16] Wolfenson H, Yang B, Sheetz MP. Steps in mechanotransduction pathways that control cell morphology. Annu Rev Physiol 2019;81:585–605. https://doi.org/10.1146/Annu.rev-physiol-021317-121245.

[17] Morgan JT, Murphy CJ, Russell P. What do mechanotransduction, Hippo, Wnt, and TGFβ have in common? YAP and TAZ as key orchestrating molecules in ocular health and disease. Exp Eye Res 2013;115:1–12. https://doi.org/10.1016/j.exer.2013.06.012.

[18] Massagué J. TGFβ in cancer. Cell 2008;134(2):215–30. https://doi.org/10.1016/j.cell.2008.07.001.

[19] David CJ, Huang Y-H, Chen M, Su J, Zou Y, Bardeesy N, et al. TGF-β tumor suppression through a lethal EMT. Cell 2016;164(5):1015–30. https://doi.org/10.1016/j.cell.2016.01.009.

[20] Seoane J, Gomis RR. TGF-β family signaling in tumor suppression and cancer progression. Cold Spring Harb Perspect Biol 2017;9(12):a022277. https://doi.org/10.1101/cshperspect.a022277.

[21] Zavadil J, Böttinger EP. TGF-beta and epithelial-to-mesenchymal transitions. Oncogene 2005;24(37):5764–74. https://doi.org/10.1038/sj.onc.1208927.

[22] Singh P, Wig J, Srinivasan R, et al. The Smad family and its role in pancreatic cancer. Indian J Cancer 2011;48(3):351. https://doi.org/10.4103/0019-509x.84939.

[23] Burotto M, Chiou VL, Lee J-M, Kohn EC. The MAPK pathway across different malignancies: a new perspective. Cancer 2014;120(22):3446–56. https://doi.org/10.1002/cncr.28864.

[24] Massagué J. TGFβ signalling in context. Nat Rev Mol Cell Biol 2012;13(10):616–30. https://doi.org/10.1038/nrm3434.

[25] Roy SK, Srivastava RK, Shankar S. Inhibition of PI3K/AKT and MAPK/ERK pathways causes activation of FOXO transcription factor, leading to cell cycle arrest and apoptosis in pancreatic cancer. J Mol Signal 2010;5(1):1–13. https://doi.org/10.1186/1750-2187-5-10.
[26] Furler RL, Nixon DF, Brantner CA, Popratiloff A, Uittenbogaart CH. TGF-β sustains tumor progression through Biochem.ical and mechanical signal transduction. Cancers 2018;10(6):199. https://doi.org/10.3390/cancers10060199.
[27] Leight JL, Wozniak MA, Chen S, Lynch ML, Chen CS. Matrix rigidity regulates a switch between TGF-β1–induced apoptosis and epithelial-mesenchymal transition. Mol Biol Cell 2012;23(5):781–91. https://doi.org/10.1091/mbc.e11-06-0537.
[28] Futakuchi M, Lami K, Tachibana Y, Yamamoto Y, Furukawa M, Fukuoka J. The effects of TGF-β signaling on cancer cells and cancer stem cells in the bone microenvironment. Int J Mol Sci 2019;20(20):5117. https://doi.org/10.3390/ijms20205117.
[29] Heldin C-H, Vanlandewijck M, Moustakas A. Regulation of EMT by TGFβ in cancer. FEBS Lett 2012;586(14):1959–70. https://doi.org/10.1016/j.febslet.2012.02.037.
[30] Wei SC, Fattet L, Tsai JH, Guo Y, Pai VH, Majeski HE, et al. Matrix stiffness drives epithelial–mesenchymal transition and tumour metastasis through a TWIST1–G3BP2 mechanotransduction pathway. Nat Cell Biol 2015;17(5):678–88. https://doi.org/10.1038/ncb3157.
[31] Schwartz MA. Integrins and extracellular matrix in mechanotransduction. Cold Spring Harb Perspect Biol 2010;2(12):a005066. https://doi.org/10.1101/cshperspect.a005066.
[32] Sieg DJ, Hauck CR, Ilic D, Klingbeil CK, Schaefer E, Damsky CH, et al. FAK integrates growth-factor and integrin signals to promote cell migration. Nat Cell Biol 2000;2(5):249–56. https://doi.org/10.1038/35010517.
[33] Guan J-L. Role of focal adhesion kinase in integrin signaling. Int J Biochem Cell Biol 1997;29(8–9):1085–96. https://doi.org/10.2741/cary.
[34] Del Rio A, Perez-Jimenez R, Liu R, Roca-Cusachs P, Fernandez JM, Sheetz MP. Stretching single talin rod molecules activates vinculin binding. Sci 2009;323(5914):638–41. https://doi.org/10.1126/Sci..1162912.
[35] Heinrichs A. Switch and stretch. Nat Rev Mol Cell Biol 2009;10(3):163. https://doi.org/10.1038/nrm2642.
[36] Sheetz MP, Felsenfeld DP, Galbraith CG. Cell migration: regulation of force on extracellular-matrix-integrin complexes. Trends Cell Biol 1998;8(2):51–4. https://doi.org/10.1016/s0962-8924(98)80005-6.
[37] Mayer IA, Arteaga CL. The PI3K/AKT pathway as a target for cancer treatment. Annu Rev Med 2016;67:11–28. https://doi.org/10.1146/Annu.rev-med-062913-051343.
[38] Yang H, Guan L, Li S, Jiang Y, Xiong N, Li L, et al. Mechanosensitive caveolin-1 activation-induced PI3K/Akt/mTOR signaling pathway promotes breast cancer motility, invadopodia formation and metastasis in vivo. Oncotarget 2016;7(13):16227. https://doi.org/10.18632/oncotarget.7583.
[39] Hood JD, Cheresh DA. Role of integrins in cell invasion and migration. Nat Rev Cancer 2002;2(2):91–100. https://doi.org/10.1038/nrc727.
[40] Burridge K, Monaghan-Benson E, Graham DM. Mechanotransduction: from the cell surface to the nucleus via RhoA. Philos Trans R Soc 2019;374(1779):20180229. https://doi.org/10.1098/rstb.2018.0229.
[41] Porta C, Paglino C, Mosca A. Targeting PI3K/Akt/mTOR signaling in cancer. Front Oncol 2014;4:64. https://doi.org/10.3389/fonc.2014.00064.
[42] Behrens J, Lustig B. The Wnt connection to tumorigenesis. Int J Dev Biol 2004;48(5–6):477–87. https://doi.org/10.1387/ijdb.041815jb.
[43] Kikuchi A, Yamamoto H, Sato A, Matsumoto S. Wnt5a: its signalling, functions and implication in diseases. Acta Physiol Scand 2012;204(1):17–33. https://doi.org/10.1111/j.1748-1716.2011.02294.x.
[44] Lustig B, Behrens J. The Wnt signaling pathway and its role in tumor dev. J Cancer Res Clin Oncol 2003;129(4):199–221. https://doi.org/10.1007/s00432-003-0431-0.
[45] Clevers H. Wnt/β-catenin signaling in development and disease. Cell 2006;127(3):469–80. https://doi.org/10.1016/j.cell.2006.10.018.
[46] Ackers I, Malgor R. Interrelationship of canonical and non-canonical Wnt signalling pathways in chronic metabolic diseases. Diab Vasc Dis Res 2018;15(1):3–13. https://doi.org/10.1177/1479164117738442.
[47] Mitte CUBCC, Berlin CU. The Piezo1 Mechanosensitive Ion Channel Promotes Melanoma Malignant Progression by Activating PI3K-AKT Signaling; 2021.
[48] Zhang S, Cao S, Gong M, Zhang W, Zhang W, Zhu Z, et al. Mechanically activated ion channel Piezo1 contributes to melanoma malignant progression through AKT/mTOR signaling. Cancer Biol Ther 2022;23(1):336–47. https://doi.org/10.1080/15384047.2022.2060015.
[49] Han Y, Liu C, Zhang D, Men H, Huo L, Geng Q, et al. Mechanosensitive ion channel Piezo1 promotes prostate cancer Dev through the activation of the Akt/mTOR pathway and acceleration of cell cycle. Int J Oncol 2019;55(3):629–44. https://doi.org/10.3892/ijo.2019.4839.
[50] Tijore A, Margadant F, Yao M, Hariharan A, Chew CAZ, Powell S, et al. Ultrasound-mediated mechanical forces selectively kill tumor cells. BioRxiv 2020.
[51] Freese JL, Pino D, Pleasure SJ. Wnt signaling in development and disease. Neurobiol Dis 2010;38(2):148–53. https://doi.org/10.1186/2045-3701-2-14.
[52] Wu B, Crampton SP, Hughes CC. Wnt signaling induces matrix metalloproteinase expression and regulates T cell transmigration. Immunity 2007;26(2):227–39. https://doi.org/10.1016/j.immuni.2006.12.007.
[53] Rubin EM, Guo Y, Tu K, Xie J, Zi X, Hoang BH. Wnt Inhibitory Factor 1 (WIF-1) decreases tumorigenesis and metastasis in osteosarcoma. Mol Cancer Ther 2010;9(3):731–41. https://doi.org/10.1158/1535-7163.MCT-09-0147.
[54] Yee DS, Tang Y, Li X, Liu Z, Guo Y, Ghaffar S, et al. The Wnt inhibitory factor 1 restoration in prostate cancer cells was associated with reduced tumor growth, decreased capacity of cell migration and invasion and a reversal of epithelial to mesenchymal transition. Mol Cancer 2010;9(1):1–14. https://doi.org/10.1186/1476-4598-9-162.
[55] Huang D, Du X. Crosstalk between tumor cells and microenvironment via Wnt pathway in colorectal cancer dissemination. World J Gastroenterol 2008;14(12):1823. https://doi.org/10.3748/wjg.14.1823.
[56] Wörthmüller J, Rüegg C. The crosstalk between FAK and Wnt signaling pathways in cancer and its therapeutic implication. Int J Mol Sci 2020;21(23):9107. https://doi.org/10.3390/ijms21239107.

[57] Wissmann C, Wild PJ, Kaiser S, Roepcke S, Stoehr R, Woenckhaus M, et al. WIF1, a component of the Wnt pathway, is down-regulated in prostate, breast, lung, and bladder cancer. The J Pathology: A J the Pathological Soc of Great Britain and Ireland 2003;201(2):204–12. https://doi.org/10.1002/path.1449.
[58] Lin Y-C, You L, Xu Z, He B, Yang C-T, Chen J-K, et al. Wnt inhibitory factor-1 gene transfer inhibits melanoma cell growth. Hum Gene Ther 2007;18(4):379–86. https://doi.org/10.1089/hum.2006.005.
[59] Boopathy GT, Hong W. Role of hippo pathway-YAP/TAZ signaling in angiogenesis. Front Cell Dev Biol 2019;7:49. https://doi.org/10.3389/fcell.2019.00049.
[60] Piccolo S, Sirio D, Cordenonsi M. The Biol of YAP/TAZ: hippo signaling and beyond. Phys Rev 2014;94(4):1287–312. https://doi.org/10.1152/physRev.00005.2014.
[61] Chang Y-C, Wu J-W, Wang C-W, Jang AC-C. Hippo signaling-mediated mechanotransduction in cell movement and cancer metastasis. Front Mol Biosci 2020;6:157. https://doi.org/10.3389/fmolb.2019.00157.
[62] Yu F-X, Guan K-L. The hippo pathway: regulators and regulations. Genes Dev 2013;27(4):355–71. https://doi.org/10.1101/gad.210773.112.
[63] Calses PC, Crawford JJ, Lill JR, Dey A. Hippo pathway in cancer: aberrant regulation and therapeutic opportunities. Trends Cancer 2019;5(5):297–307. https://doi.org/10.1016/j.trecan.2019.04.001.
[64] Kim W, Jho E-h. The history and regulatory mechanism of the Hippo pathway. BMB Rep 2018;51(3):106. https://doi.org/10.5483/bmbrep.2018.51.3.022.
[65] Calvo F, Ege N, Grande-Garcia A, Hooper S, Jenkins RP, Chaudhry SI, et al. Mechanotransduction and YAP-dependent matrix remodelling is required for the generation and maintenance of cancer-associated fibroblasts. Nat Cell Biol 2013;15(6):637–46. https://doi.org/10.1038/ncb2756.
[66] Cai X, Wang K-C, Meng Z. Mechanoregulation of YAP and TAZ in cellular homeostasis and disease progression. Front Cell Dev Biol 2021;9:673599. https://doi.org/10.3389/fcell.2021.673599.
[67] Dupont S, Morsut L, Aragona M, Enzo E, Giulitti S, Cordenonsi M, et al. Role of YAP/TAZ in mechanotransduction. Nat 2011;474(7350):179–83. https://doi.org/10.1038/Nat.10137.
[68] Hao J, Zhang Y, Jing D, Li Y, Li J, Zhao Z. Role of Hippo signaling in cancer stem cells. J Cell Physiol 2014;229(3):266–70. https://doi.org/10.14348/molcells.2018.2242.
[69] Thompson BJ. YAP/TAZ: drivers of tumor growth, metastasis, and resistance to therapy. BioEssays 2020;42(5):1900162. https://doi.org/10.1002/bies.201900162.
[70] Elbediwy A, Vincent-Mistiaen ZI, Thompson BJ. YAP and TAZ in epithelial stem cells: a sensor for cell polarity, mechanical forces and tissue damage. BioEssays 2016;38(7):644–53. https://doi.org/10.1002/bies.201600037.
[71] Warren JS, Xiao Y, Lamar JM. YAP/TAZ activation as a target for treating metastatic cancer. Cancers 2018;10(4):115. https://doi.org/10.3390/cancers10040115.
[72] Bouvier C, Macagno N, Nguyen Q, Loundou A, Jiguet-Jiglaire C, Gentet J-C, et al. Prognostic value of the Hippo pathway transcriptional coactivators YAP/TAZ and β1-integrin in conventional osteosarcoma. Oncotarget 2016;7(40):64702. https://doi.org/10.18632/oncotarget.11876.
[73] Sanchez P, Clement V, Ruiz i Altaba A. Therapeutic targeting of the Hedgehog-GLI pathway in prostate cancer. Cancer Res 2005;65(8):2990–2. https://doi.org/10.1158/0008-5472.can-05-0439.
[74] Cohen Jr MM. The hedgehog signaling network. Am J Med Genet, Part A 2003;123(1):5–28. https://doi.org/10.1002/ajmg.a.20495.
[75] Heller E, Hurchla MA, Xiang J, Su X, Chen S, Schneider J, et al. Hedgehog signaling inhibition blocks growth of resistant tumors through effects on tumor microenvironment. Cancer Res 2012;72(4):897–907. https://doi.org/10.1158/0008-5472.can-11-2681.
[76] Jiang J, Hui C-c. Hedgehog signaling in dev and cancer. Dev Cell 2008;15(6):801–12. https://doi.org/10.1016/j.devcel.2008.11.010.
[77] Verbeni M, Sánchez O, Mollica E, Siegl-Cachedenier I, Carleton A, Guerrero I, et al. Morphogenetic action through flux-limited spreading. Phys Life Rev 2013;10(4):457–75. https://doi.org/10.1016/j.plRev.2013.06.004.
[78] Ahmad A, Maitah MY, Ginnebaugh KR, Li Y, Bao B, Gadgeel SM, et al. Inhibition of Hedgehog signaling sensitizes NSCLC cells to standard therapies through modulation of EMT-regulating miRNAs. J Hematol Oncol 2013;6(1):1–10. https://doi.org/10.1186/1756-8722-6-77.
[79] Katoh Y, Katoh M. Hedgehog signaling, epithelial-to-mesenchymal transition and miRNA. Int J Mol Med 2008;22(3):271–5. https://doi.org/10.3892/ijmm_00000019.
[80] Li Y, Maitah MY, Ahmad A, Kong D, Bao B, Sarkar FH. Targeting the Hedgehog signaling pathway for cancer therapy. Expert Opin Ther Targets 2012;16(1):49–66. https://doi.org/10.1177/1758834010366430.
[81] Song L, Li Z-Y, Liu W-P, Zhao M-R. Crosstalk between Wnt/β-catenin and Hedgehog/Gli signaling pathways in colon cancer and implications for therapy. Cancer Biol Ther 2015;16(1):1–7. https://doi.org/10.4161/15384047.2014.972215.
[82] Javelaud D, Pierrat M-J, Mauviel A. Crosstalk between TGF-β and hedgehog signaling in cancer. FEBS Lett 2012;586(14):2016–25. https://doi.org/10.1016/j.febslet.2012.05.011.
[83] Yoo YA, Kang MH, Lee HJ, Kim B-h, Park JK, Kim HK, et al. Sonic hedgehog pathway promotes metastasis and lymphangiogenesis via activation of Akt, EMT, and MMP-9 pathway in gastric cancer. Cancer Res 2011;71(22):7061–70. https://doi.org/10.1158/0008-5472.CAN-11-1338.
[84] Brechbiel J, Miller-Moslin K, Adjei AA. Crosstalk between hedgehog and other signaling pathways as a basis for combination therapies in cancer. Cancer Treat Rev 2014;40(6):750–9. https://doi.org/10.1016/j.ctrv.2014.02.003.
[85] Aguirre-Tamaral A, Cambón M, Poyato D, Soler J, Guerrero I. Predictive model for cytoneme guidance in Hedgehog signaling based on Ihog-Glypicans interaction. Nat Commun 2022;13(1):1–14. https://doi.org/10.1038/s41467-022-33262-4.
[86] Qi Y, Liu H, Zhang K, Wu Y, Shen C, Lin X. Ihog proteins contribute to integrin-mediated focal adhesions. Sci China Life Sci 2022:1–10. https://doi.org/10.1007/s11427-022-2154-1.
[87] Muz B, de la Puente P, Azab F, Azab AK. The role of hypoxia in cancer progression, angiogenesis, metastasis, and resistance to therapy. Hypoxia 2015;3:83. https://doi.org/10.2147/HP.S93413.

[88] Hockel M, Vaupel P. Tumor hypoxia: definitions and curr clinical, biologic and molecular aspects. J Natl Cancer Inst 2001;93(4):266–76. https://doi.org/10.1093/jnci/93.4.266.
[89] Vaupel P. The role of hypoxia-induced factors in tumor progression. The Oncologist 2004;9(S5):10–7. https://doi.org/10.1634/theoncologist.9-90005-10.
[90] Höckel M, Vaupel P. Biological consequences of tumor hypoxia. Semin Oncol, vol. 28. Elsevier; 2001. p. 36–41. https://pubmed.ncbi.nlm.nih.gov/11395851/.
[91] Kerbel RS. Tumor angiogenesis. N Engl J Med 2008;358(19):2039–49. https://doi.org/10.1056/nejmra0706596.
[92] Folkman J. Tumor angiogenesis: therapeutic implications. N Engl J Med 1971;285(21):1182–6. https://doi.org/10.1056/nejm197111182852108.
[93] Arneth B. Tumor microenvironment. Medicina 2019;56(1):15. https://doi.org/10.3390/medicina56010015.
[94] Whiteside T. The tumor microenvironment and its role in promoting tumor growth. Oncogene 2008;27(45):5904–12. https://doi.org/10.1038/onc.2008.271.
[95] Roose T, Netti PA, Munn LL, Boucher Y, Jain RK. Solid stress generated by spheroid growth estimated using a linear poroelasticity model. Microvasc Res 2003;66(3):204–12. https://doi.org/10.1016/s0026-2862(03)00057-8.
[96] Blanco B, Campos J, Melchor J, Soler J. Modeling interactions among migration, growth and pressure in tumor dynamics. Math 2021;9(12):1376. https://doi.org/10.3390/math9121376.
[97] Ranft J, Aliee M, Prost J, Jülicher F, Joanny J-F. Mechanically driven interface propagation in biological tissues. New J Phys 2014;16(3):035002. https://doi.org/10.1088/1367-2630/16/3/035002.
[98] Shraiman BI. Mechanical feedback as a possible regulator of tissue growth. Proc Natl Acad Sci 2005;102(9):3318–23. https://doi.org/10.1073/pnas.0404782102.
[99] Roca-Cusachs P, Conte V, Trepat X. Quantifying forces in cell biol. Nat Cell Biol 2017;19(7):742–51. https://doi.org/10.1038/ncb3564.
[100] Helmlinger G, Netti PA, Lichtenbeld HC, Melder RJ, Jain RK. Solid stress inhibits the growth of multicellular tumor spheroids. Nat Biotechnol 1997;15(8):778. https://doi.org/10.1038/nbt0897-778.
[101] Cheng G, Tse J, Jain RK, Munn LL. Micro-environmental mechanical stress controls tumor spheroid size and morphology by suppressing proliferation and inducing apoptosis in cancer cells. PLoS ONE 2009;4(2):e4632. https://doi.org/10.1371/journal.pone.0004632.
[102] Montel F, Delarue M, Elgeti J, Vignjevic D, Cappello G, Prost J. Isotropic stress reduces cell proliferation in tumor spheroids. New J Phys 2012;14(5):055008. https://doi.org/10.1088/1367-2630/14/5/055008.
[103] Delarue M, Montel F, Vignjevic D, Prost J, Joanny J-F, Cappello G. Compressive stress inhibits proliferation in tumor spheroids through a volume limitation. Biophys J 2014;107(8):1821–8. https://doi.org/10.1016/j.bpj.2014.08.031.
[104] Mascheroni P, Stigliano C, Carfagna M, Boso DP, Preziosi L, Decuzzi P, et al. Predicting the growth of glioblastoma multiforme spheroids using a multiphase porous media model. Biomech Model Mechanobiol 2016;15(5):1215–28.
[105] Bonnet-Gonnet C, Belloni L, Cabane B. Osmotic pressure of latex dispersions. Langmuir 1994;10(11):4012–21. https://doi.org/10.1021/la00023a019.
[106] Janet MT, Cheng G, Tyrrell JA, Wilcox-Adelman SA, Boucher Y, Jain RK, et al. Mechanical compression drives cancer cells toward invasive phenotype. Proc Natl Acad Sci 2012;109(3):911–6. https://doi.org/10.1073/pnas.1118910109.
[107] González I, Luzuriaga J, Valdivieso A, Frutos J, López J, Hernández L, et al. Low-intensity ultrasound inhibits the long-term migration of cancer cells; 2021.
[108] Alessandri K, Sarangi BR, Gurchenkov VV, Sinha B, Kießling TR, Fetler L, et al. Cellular capsules as a tool for multicellular spheroid production and for investigating the mechanics of tumor progression in vitro. Proc Natl Acad Sci 2013;110(37):14843–8. https://doi.org/10.1073/pnas.1309482110.
[109] Kalli M, Stylianopoulos T. Defining the role of solid stress and matrix stiffness in cancer cell proliferation and metastasis. Front Oncol 2018;8:55. https://doi.org/10.3389/fonc.2018.00055.
[110] Nagelkerke A, Bussink J, Rowan AE, Span PN. The mechanical microenvironment in cancer: how phys affects tumours. Semin Cancer Biol 2015;35:62–70. https://doi.org/10.1016/j.semcancer.2015.09.001. Elsevier.
[111] Stylianopoulos T, Martin JD, Chauhan VP, Jain SR, Diop-Frimpong B, Bardeesy N, et al. Causes, consequences, and remedies for growth-induced solid stress in murine and human tumors. Proc Natl Acad Sci 2012;109(38):15101–8. https://doi.org/10.1073/pnas.1213353109.
[112] Stylianopoulos T. The solid mechanics of cancer and strategies for improved therapy. J Biomech Eng 2017;139(2).
[113] Chauhan VP, Boucher Y, Ferrone CR, Roberge S, Martin JD, Stylianopoulos T, et al. Compression of pancreatic tumor blood vessels by hyaluronan is caused by solid stress and not interstitial fluid pressure. Cancer Cell 2014;26(1):14. https://doi.org/10.1016/j.ccr.2014.06.003.
[114] Ariffin AB, Forde PF, Jahangeer S, Soden DM, Hinchion J. Releasing pressure in tumors: what do we know so far and where do we go from here? A Rev Cancer Res 2014;74(10):2655–62. https://doi.org/10.1158/0008-5472.can-13-3696.
[115] Jain RK, Martin JD, Stylianopoulos T. The role of mechanical forces in tumor growth and therapy. Annu Rev Biomed Eng 2014;16:321–46. https://doi.org/10.1146/Annu.rev-bioeng-071813-105259.
[116] Ramírez-Torres A, Rodríguez-Ramos R, Merodio J, Penta R, Bravo-Castillero J, Guinovart-Díaz R, et al. The influence of anisotropic growth and geometry on the stress of solid tumors. Int J Eng Sci 2017;119:40–9. https://doi.org/10.1016/j.ijengsci.2017.06.011.
[117] Collins C, Denisin AK, Pruitt BL, Nelson WJ. Changes in e-cadherin rigidity sensing regulate cell adhesion. Proc Natl Acad Sci 2017;114(29):E5835–44. https://doi.org/10.1073/pnas.1618676114.
[118] Basan M, Risler T, Joanny J-F, Sastre-Garau X, Prost J. Homeostatic competition drives tumor growth and metastasis nucleation. HFSP J 2009;3(4):265–72. https://doi.org/10.2976/1.3086732.
[119] Ranft J, Basan M, Elgeti J, Joanny J-F, Prost J, Jülicher F. Fluidization of tissues by cell division and apoptosis. Proc Natl Acad Sci 2010;107(49):20863–8. https://doi.org/10.1073/pnas.1011086107.
[120] Casas-Tintó S, Portela M. Cytonemes, their formation, regulation, and roles in signaling and communication in tumorigenesis. Int J Mol Sci 2019;20(22):5641. https://doi.org/10.3390/ijms20225641.

[121] Sunyer R, Trepat Durotaxis X. Curr Biol 2020;30(9):R383–7. https://doi.org/10.1016/j.cub.2020.03.051.
[122] Rens EG, Merks RM. Cell shape and durotaxis explained from cell-extracellular matrix forces and focal adhesion dynamics. iScience 2020;23(9):101488. https://doi.org/10.1016/j.isci.2020.101488.
[123] Yeoman B, Shatkin G, Beri P, Banisadr A, Katira P, Engler AJ. Adhesion strength and contractility enable metastatic cells to become adurotactic. Cell Rep 2021;34(10):108816. https://doi.org/10.1016/j.celrep.2021.108816.
[124] Harland B, Walcott S, Sun SX. Adhesion dynamics and durotaxis in migrating cells. Phys Biol 2011;8(1):015011. https://doi.org/10.1088/1478-3975/8/1/015011.
[125] Panzetta V, Fusco S, Netti PA. Cell mechanosensing is regulated by substrate strain energy rather than stiffness. Proc Natl Acad Sci 2019;116(44):22004–13. https://doi.org/10.1073/pnas.1904660116.
[126] Munn LL, Nia HT. Mechanosensing tensile solid stresses. Proc Natl Acad Sci 2019;116(44):21960–2. https://doi.org/10.1073/pnas.1916115116.
[127] Lorenzo G, Hughes TJ, Dominguez-Frojan P, Reali A, Gomez H. Computer simulations suggest that prostate enlargement due to benign prostatic hyperplasia mechanically impedes prostate cancer growth. Proc Natl Acad Sci 2019;116(4):1152–61. https://doi.org/10.1073/pnas.1815735116.
[128] Stylianopoulos T, Munn LL, Jain RK. Reengineering the physical microenvironment of tumors to improve drug delivery and efficacy: from mathematical modeling to bench to bedside. Trends Cancer 2018;4(4):292–319. https://doi.org/10.1016/j.trecan.2018.02.005.
[129] Voutouri C, Stylianopoulos T. Accumulation of mechanical forces in tumors is related to hyaluronan content and tissue stiffness. PLoS ONE 2018;13(3):e0193801. https://doi.org/10.1371/journal.pone.0193801.
[130] Skalak R, Zargaryan S, Jain RK, Netti PA, Hoger A. Compatibility and the genesis of residual stress by volumetric growth. J Math Biol 1996;34(8):889–914. https://doi.org/10.1007/BF01834825.
[131] Ambrosi D, Pezzuto S, Riccobelli D, Stylianopoulos T, Ciarletta P. Solid tumors are poroelastic solids with a chemo-mechanical feedback on growth. J Elast 2017;129(1–2):107–24. https://doi.org/10.1007/978-94-024-1220-8_6.
[132] Nia H, Liu H, Seano G, Datta M, Jones D, Rahbari N, et al. Solid stress and elastic energy as measures of tumor mechanopathology. Nat Biomed Eng 2017;1(0004). https://doi.org/10.1038/s41551-016-0004.
[133] Huang Q, Hu X, He W, Zhao Y, Hao S, Wu Q, et al. Fluid shear stress and tumor metastasis. Am J Cancer Res 2018;8(5):763. https://pubmed.ncbi.nlm.nih.gov/29888101/.
[134] Barnes JM, Nauseef JT, Henry MD. Resistance to fluid shear stress is a conserved biophysical property of malignant cells. PLoS ONE 2012;7(12):e50973. https://doi.org/10.1371/journal.pone.0050973.
[135] Shieh AC, Swartz MA. Regulation of tumor invasion by interstitial fluid flow. Phys Biol 2011;8(1):015012. https://doi.org/10.1088/1478-3975/8/1/015012s.
[136] Tsuji T, Ibaragi S, Hu G-f. Epithelial-mesenchymal transition and cell cooperativity in metastasis. Cancer Res 2009;69(18):7135–9. https://doi.org/10.1158/0008-5472.can-09-1618.
[137] Stylianopoulos T, Martin JD, Snuderl M, Mpekris F, Jain SR, Jain RK. Coevolution of solid stress and interstitial fluid pressure in tumors during progression: implications for vascular collapse. Cancer Res 2013;73(13):3833–41. https://doi.org/10.1158/0008-5472.can-12-4521f.
[138] Wirtz D, Konstantopoulos K, Searson PC. The phys of cancer: the role of physical interactions and mechanical forces in metastasis. Nat Rev Cancer 2011;11(7):512–22. https://doi.org/10.1038/nrc3080.
[139] Gray KM, Stroka KM. Vascular endothelial cell mechanosensing: new insights gained from biomimetic microfluidic models. Semin Cell Dev Biol 2017;71:106–17. https://doi.org/10.1016/j.semcdb.2017.06.002. Elsevier.
[140] Liu LJ, Brown SL, Ewing JR, Ala BD, Schneider KM, Schlesinger M. Estimation of tumor interstitial fluid pressure (TIFP) noninvasively. PLoS ONE 2016;11(7):e0140892. https://doi.org/10.1371/journal.pone.0140892.
[141] Nathan SS, DiResta GR, Casas-Ganem JE, Hoang BH, Sowers R, Yang R, et al. Elevated physiologic tumor pressure promotes proliferation and chemosensitivity in human osteosarcoma. Clin Cancer Res 2005;11(6):2389–97. https://doi.org/10.1158/1078-0432.ccr-04-2048.
[142] Hofmann M, Guschel M, Bernd A, Bereiter-Hahn J, Kaufmann R, Tandi C, et al. Lowering of tumor interstitial fluid pressure reduces tumor cell proliferation in a xenograft tumor model. Neoplasia 2006;8(2):89–95. https://doi.org/10.1593/neo.05469.
[143] Kim H-g, Yu AR, Lee JJ, Lee Y-J, Lim SM, Kim JS. Measurement of tumor pressure and strategies of imaging tumor pressure for radioimmunotherapy. Eur J Nucl Med Mol Imaging 2019:1–7. https://doi.org/10.1007/s13139-019-00598-7.
[144] Markl M, Wallis W, Harloff A. Reproducibility of flow and wall shear stress analysis using flow-sensitive four-dimensional MRI. J Magn Reson Imaging 2011;33(4):988–94. https://doi.org/10.1002/jmri.22519.
[145] Potters WV, Marquering HA, VanBavel E, Nederveen AJ. Measuring wall shear stress using velocity-encoded MRI. Curr Cardiovasc Imaging Rep 2014;7(4):1–12. https://doi.org/10.1007/s12410-014-9257-1.
[146] Seano G, Nia HT, Emblem KE, Datta M, Ren J, Krishnan S, et al. Solid stress in brain tumours causes neuronal loss and neurological dysfunction and can be reversed by lithium. Nat Biomed Eng 2019;3(3):230. https://doi.org/10.1038/s41551-018-0334-7.
[147] Follain G, Herrmann D, Harlepp S, Hyenne V, Osmani N, Warren SC, et al. Fluids and their mechanics in tumour transit: shaping metastasis. Nat Rev Cancer 2020;20(2):107–24. https://doi.org/10.1038/s41568-019-0221-x.
[148] Lorenzo G, Hughes T, Reali A, Gomez H. A numerical simulation study of the dual role of 5α-reductase inhibitors on tumor growth in prostates enlarged by benign prostatic hyperplasia via stress relaxation and apoptosis upregulation. Comput Methods Appl Mech Eng 2020;362:112843. https://doi.org/10.1016/j.cma.2020.112843.
[149] Nandalur KR, Colvin R, Walker D, Nandalur SR, Seifman B, Gangwish D, et al. Benign prostate hyperplasia as a potential protective factor against prostate cancer: insights from a magnetic resonance imaging study of compositional characteristics. Prostate 2021;81(14):1097–104. https://doi.org/10.1002/pros.24207.
[150] Sinkus R, Tanter M, Xydeas T, Catheline S, Bercoff J, Fink M. Viscoelastic shear properties of in vivo breast lesions measured by MR elastography. Magn Reson Imaging 2005;23(2):159–65. https://doi.org/10.1016/j.mri.2004.11.060.

[151] Alibert C, Goud B, Manneville J-B. Are cancer cells really softer than normal cells? Cell Biol 2017;109(5):167–89. https://doi.org/10.1111/boc.201600078.
[152] Masuzaki R, Tateishi R, Yoshida H, Sato T, Ohki T, Goto T, et al. Assessing liver tumor stiffness by transient elastography. Hepatol Int 2007;1(3):394–7. https://doi.org/10.1007/s12072-007-9012-7.
[153] Barr RG, Memo R, Schaub CR. Shear wave ultrasound elastography of the prostate: initial results. Ultrasound Q 2012;28(1):13–20. https://doi.org/10.1097/ruq.0b013e318249f594.
[154] Murphy MC, Huston J, Glaser KJ, Manduca A, Meyer FB, Lanzino G, et al. Preoperative assessment of meningioma stiffness using magnetic resonance elastography. J Neurosurg 2013;118(3):643–8. https://doi.org/10.3171/2012.9.jns12519.
[155] Efremov YM, Velay-Lizancos M, Weaver CJ, Athamneh AI, Zavattieri PD, Suter DM, et al. Anisotropy vs isotropy in living cell indentation with AFM. Sci Rep 2019;9(1):1–12. https://doi.org/10.1038/s41598-019-42077-1.
[156] Lim C, Zhou E, Quek S. Mechanical models for living cells?a rev. J Biomech 2006;39(2):195–216. https://doi.org/10.1016/j.jbiomech.2004.12.008.
[157] Pepin KM, McGee KP. Quantifying tumor stiffness with magnetic resonance elastography: the role of mechanical properties for detection, characterization, and treatment stratification in oncol. Top Magn Reson Imaging 2018;27(5):353–62. https://doi.org/10.1097/rmr.0000000000000181.
[158] Bohte A, Nelissen J, Runge J, Holub O, Lambert S, de Graaf L, et al. Breast magnetic resonance elastography: a rev of clinical work and future perspectives. NMR Biomed 2018;31(10):e3932. https://doi.org/10.1002/nbm.3932.
[159] Streitberger K-J, Lilaj L, Schrank F, Braun J, Hoffmann K-T, Reiss-Zimmermann M, et al. How tissue fluidity influences brain tumor progression. Proc Natl Acad Sci 2020;117(1):128–34. https://doi.org/10.1073/pnas.1913511116.
[160] Elosegui-Artola A. The extracellular matrix viscoelasticity as a regulator of cell and tissue dynamics. Curr Opin Cell Biol 2021;72:10–8. https://doi.org/10.1016/j.ceb.2021.04.002.
[161] Elosegui-Artola A, Gupta A, Najibi AJ, Seo BR, Garry R, Darnell M, et al. Matrix viscoelasticity controls spatio-temporal tissue organization. Nat Mater 2022. https://doi.org/10.1038/s41563-022-01400-4.
[162] Saffman PG, Taylor GI. The penetration of a fluid into a porous medium or hele-shaw cell containing a more viscous liquid. Proc R Soc Lond Ser A, Math Phys Sci 1958;245(1242):312–29. https://doi.org/10.1098/rspa.1958.0085.
[163] Homsy GM. Viscous fingering in porous media. Annu Rev Fluid Mech 1987;19(1):271–311. https://doi.org/10.1146/Annu.Rev.fl.19.010187.001415.
[164] Streitberger K-J, Reiss-Zimmermann M, Freimann FB, Bayerl S, Guo J, Arlt F, et al. High-resolution mechanical imaging of glioblastoma by multifrequency magnetic resonance elastography. PLoS ONE 2014;9(10):e110588. https://doi.org/10.1371/journal.pone.0110588.
[165] Conte M, Casas-Tintò S, Soler J. Modeling invasion patterns in the glioblastoma battlefield. PLoS Comput Biol 2021;17(1):e1008632. https://doi.org/10.1371/journal.pcbi.1008632.
[166] Conte M, Surulescu C. Mathematical modeling of glioma invasion: acid-and vasculature mediated go-or-grow dichotomy and the influence of tissue anisotropy. Appl Math Comput 2021;407:126305.
[167] Pérez-García VM, Bogdanska M, Martínez-González A, Belmonte-Beitia J, Schucht P, Pérez-Romasanta LA. Delay effects in the response of low-grade gliomas to radiotherapy: a mathematical model and its therapeutical implications. Math Med Biol 2015;32(3):307–29. https://doi.org/10.1093/imammb/dqu009.
[168] Metzcar J, Wang Y, Heiland R, Macklin P. A rev of cell-based computational modeling in cancer biol. JCO Clin Cancer Inf 2019;2:1–13. https://doi.org/10.1200/CCI.18.00069.
[169] Rodriguez EK, Hoger A, McCulloch AD. Stress-dependent finite growth in soft elastic tissues. J Biomech 1994;27(4):455–67. https://doi.org/10.1016/0021-9290(94)90021-3.
[170] Rajagopal KR, Tao L. Mechanics of mixtures, vol. 35. World Scientific; 1995.
[171] Taber LA. Biomechanics of growth, remodeling, and morphogenesis. Appl Mech Rev 1995;48(8):487. https://doi.org/10.1115/1.3005109.
[172] Ambrosi D, Mollica F. On the mechanics of a growing tumor. Int J Eng Sci 2002;40(12):1297–316. https://doi.org/10.1016/S0020-7225(02)00014-9.
[173] Ambrosi D, Preziosi L. On the closure of mass balance models for tumor growth. Math Models Methods Appl Sci 2002;12(05):737–54. https://doi.org/10.1142/S0218202502001878.
[174] Araujo RP, McElwain DS. A history of the study of solid tumour growth: the contribution of mathematical modelling. Bull Math Biol 2004;66(5):1039–91. https://doi.org/10.1016/j.bulm.2003.11.002.
[175] Landau LD, Lifšic EM, Lifshitz EM, Kosevich AM, Pitaevskii LP. Theory of elasticity, vol. 7. Elsevier; 1986.
[176] Taber LA. Continuum modeling in mechanobiology. Springer; 2020.
[177] Voutouri C, Mpekris F, Papageorgis P, Odysseos AD, Stylianopoulos T. Role of constitutive behavior and tumor-host mechanical interactions in the state of stress and growth of solid tumors. PLoS ONE 2014;9(8):104717. https://doi.org/10.1371/journal.pone.0104717.
[178] Epstein M. Mathematical characterization and identification of remodeling, growth, aging and morphogenesis. J Mech Phys Solids 2015;84:72–84. https://doi.org/10.1016/j.jmps.2015.07.009.
[179] Albano G, Giorno V. A stochastic model in tumor growth. J Theor Biol 2006;242(2):329–36. https://doi.org/10.1016/j.jtbi.2006.03.001.
[180] Mpekris F, Voutouri C, Papageorgis P, Stylianopoulos T. Stress alleviation strategy in cancer treatment: insights from a mathematical model. Z Angew Math Mech 2018;98(12):2295–306. https://doi.org/10.1002/zamm.201700270.
[181] Voutouri C, Stylianopoulos T. Evolution of osmotic pressure in solid tumors. J Biomech 2014;47(14):3441–7. https://doi.org/10.1016/j.jbiomech.2014.09.019.
[182] Mpekris F, Angeli S, Pirentis AP, Stylianopoulos T. Stress-mediated progression of solid tumors: effect of mechanical stress on tissue oxygenation, cancer cell proliferation, and drug delivery. Biomech Model Mechanobiol 2015;14(6):1391–402. https://doi.org/10.1007/s10237-015-0682-0.

[183] Ciarletta P, Ambrosi D, Maugin G, Preziosi L. Mechano-transduction in tumour growth modelling. Eur Phys J E 2013;36:1–9. https://doi.org/10.1140/epje/i2013-13023-2.
[184] Byrne H, Preziosi L. Modelling solid tumour growth using the theory of mixtures. Math Med Biol 2003;20(4):341–66. https://doi.org/10.1093/imammb/20.4.341.
[185] Humphrey J, Rajagopal K. A constrained mixture model for growth and remodeling of soft tissues. Math Models Methods Appl Sci 2002;12(03):407–30. https://doi.org/10.1142/S0218202502001714.
[186] Truesdell C. Sulle basi della termomeccanica. Rend Lincei 1957;22(8):33–8.
[187] Carotenuto A, Cutolo A, Petrillo A, Fusco R, Arra C, Sansone M, et al. Growth and in vivo stresses traced through tumor mechanics enriched with predator-prey cells dynamics. J Mech Behav Biomed Mater 2018;86:55–70. https://doi.org/10.1016/j.jmbbm.2018.06.011.
[188] Carotenuto AR, Cutolo A, Palumbo S, Fraldi M. Lyapunov stability of competitive cells dynamics in tumor mechanobiol. Acta Mech Sin 2021;37(2):244–63. https://doi.org/10.1007/s10409-021-01061-7.
[189] Fraldi M, Carotenuto AR. Cells competition in tumor growth poroelasticity. J Mech Phys Solids 2018;112:345–67. https://doi.org/10.1016/j.jmps.2017.12.015.
[190] Hormuth DA, Weis JA, Barnes SL, Miga MI, Rericha EC, Quaranta V, et al. A mechanically coupled reaction–diffusion model that incorporates intra-tumoural heterogeneity to predict in vivo glioma growth. J R Soc Interface 2017;14(128):20161010. https://doi.org/10.1098/rsif.2016.1010.
[191] Casas-Vázquez J, Jou D. Nonequilibrium temperature versus local-equilibrium temperature. Phys Rev E 1994;49(2):1040. https://doi.org/10.1103/PhysRevE.49.1040.
[192] Vázquez JL. The porous medium equation: mathematical theory. Oxford University Press; 2007.
[193] Dębiec T, Perthame B, Schmidtchen M, Vauchelet N. Incompressible limit for a two-species model with coupling through brinkman's law in any dimension. J Math Pures Appl 2021;145:204–39. https://doi.org/10.1016/j.matpur.2020.11.002.
[194] Donatelli D, Trivisa K. On a nonlinear model for tumor growth: global in time weak solutions. J Math Fluid Mech 2014;16(4):787–803. https://doi.org/10.1007/s00021-014-0180-7.
[195] Calvo J, Campos J, Caselles V, Sánchez O, Soler J. Pattern formation in a flux limited reaction–diffusion equation of porous media type. Invent Math 2016;206(1):57–108. https://doi.org/10.1007/s00222-016-0649-5.
[196] Campos J, Soler J. Qualitative behavior and traveling waves for flux-saturated porous media equations arising in optimal mass transportation. Nonlinear Anal 2016;137:266–90. https://doi.org/10.1016/j.na.2015.12.021.
[197] Calvo J, Campos J, Caselles V, Sánchez Ó, Soler J. Flux-saturated porous media equations and applications. EMS Surv Math Sci 2015;2(1):131–218. https://doi.org/10.4171/emss/11.
[198] Calvo J, Campos J, Caselles V, Sánchez Ó, Soler J. Qualitative behaviour for flux-saturated mechanisms: travelling waves, waiting time and smoothing effects. J Math Biol 2017;19(2):441–72. https://doi.org/10.4171/jems/670.
[199] Campos J, Guerrero P, Sánchez Ó, Soler J. On the analysis of traveling waves to a nonlinear flux limited reaction–diffusion equation. Ann Inst H Poincaré Anal Non Linéaire 2013;30:141–55. https://doi.org/10.1016/j.anihpc.2012.07.001.
[200] Yin S-F, Xue S-L, Li B, Feng X-Q. Bio–chemo–mechanical modeling of growing biological tissues: finite element method. Int J Non-Linear Mech 2019;108:46–54. https://doi.org/10.1016/j.ijnonlinmec.2018.10.004.
[201] Ramírez-Torres A, Rodríguez-Ramos R, Glüge R, Bravo-Castillero J, Guinovart-Díaz R, Rodríguez-Sanchez R. Biomechanic approach of a growing tumor. Mech Res Commun 2013;51:32–8. https://doi.org/10.1016/j.mechrescom.2013.04.006.
[202] Ramírez-Torres A, Rodríguez-Ramos R, Merodio J, Bravo-Castillero J, Guinovart-Díaz R, Alfonso JCL. Action of body forces in tumor growth. Int J Eng Sci 2015;89:18–34. https://doi.org/10.1016/j.ijengsci.2014.11.009.
[203] Hogea C, Davatzikos C, Biros G. An image-driven parameter estimation problem for a reaction–diffusion glioma growth model with mass effects. J Math Biol 2008;56(6):793–825. https://doi.org/10.1007/s00285-007-0139-x.
[204] Chen X, Summers RM, Yao J. Kidney tumor growth prediction by coupling reaction–diffusion and biomechanical model. IEEE Trans Biomed Eng 2012;60(1):169–73. https://doi.org/10.1109/TBME.2012.2222027.
[205] Biot MA. General theory of three-dimensional consolidation. J Appl Phys 1941;12(2):155–64. https://doi.org/10.1063/1.1712886.
[206] Detournay E, Cheng AH-D. Fundamentals of poroelasticity. In: Analysis and design methods. Elsevier; 1993. p. 113–71.
[207] Cowin SC, Doty SB. Tissue mechanics. Springer; 2007.
[208] Jain RK, Tong RT, Munn LL. Effect of vascular normalization by antiangiogenic therapy on interstitial hypertension, peritumor edema, and lymphatic metastasis: insights from a mathematical model. Cancer Res 2007;67(6):2729–35. https://doi.org/10.1158/0008-5472.can-06-4102.
[209] Hormuth DA, Phillips CM, Wu C, Lima EA, Lorenzo G, Jha PK, et al. Biologically-based mathematical modeling of tumor vasculature and angiogenesis via time-resolved imaging data. Cancers 2021;13(12):3008. https://doi.org/10.3390/cancers13123008.
[210] Wu M, Frieboes HB, Chaplain MA, McDougall SR, Cristini V, Lowengrub JS. The effect of interstitial pressure on therapeutic agent transport: coupling with the tumor blood and lymphatic vascular systems. J Theor Biol 2014;355:194–207. https://doi.org/10.1016/j.jtbi.2014.04.012.
[211] Mascheroni P, Carfagna M, Grillo A, Boso D, Schrefler B. An avascular tumor growth model based on porous media mechanics and evolving natural states. Math Mech Solids 2018;23(4):686–712. https://doi.org/10.1177/1081286517711217.
[212] Xue S-L, Li B, Feng X-Q, Gao H. Biochemechanical poroelastic theory of avascular tumor growth. J Mech Phys Solids 2016;94:409–32. https://doi.org/10.1016/j.jmps.2016.05.011.
[213] Lorenzo G, Scott MA, Tew K, Hughes TJ, Zhang YJ, Liu L, et al. Tissue-scale, personalized modeling and simulation of prostate cancer growth. Proc Natl Acad Sci 2016;113(48):E7663–71. https://doi.org/10.1073/pnas.1615791113.
[214] Weis JA, Miga MI, Arlinghaus LR, Li X, Chakravarthy AB, Abramson V, et al. A mechanically coupled reaction–diffusion model for predicting the response of breast tumors to neoadjuvant chemotherapy. Phys Med Biol 2013;58(17):5851. https://doi.org/10.1088/0031-9155/58/17/5851.

[215] Jarrett AM, Hormuth DA, Barnes SL, Feng X, Huang W, Yankeelov TE. Incorporating drug delivery into an imaging-driven, mechanics-coupled reaction diffusion model for predicting the response of breast cancer to neoadjuvant chemotherapy: theory and preliminary clinical results. Phys Med Biol 2018;63(10):105015. https://doi.org/10.1088/1361-6560/aac040.
[216] Ambrosi D, Preziosi L. Cell adhesion mechanisms and stress relaxation in the mechanics of tumours. Biomech Mod Mechanbiol 2009;8(5):397. https://doi.org/10.1007/s10237-008-0145-y.
[217] Chaplain MA, Graziano L, Preziosi L. Mathematical modelling of the loss of tissue compression responsiveness and its role in solid tumour dev. Math Med Biol 2006;23(3):197–229. https://doi.org/10.1093/imammb/dql009.
[218] Wood AK, Sehgal CM. A rev of low-intensity ultrasound for cancer therapy. Ultrasound Med Biol 2015;41(4):905–28. https://doi.org/10.1016/j.ultrasmedbio.2014.11.019.
[219] Mittelstein DR, Ye J, Schibber EF, Roychoudhury A, Martinez LT, Fekrazad MH, et al. Selective ablation of cancer cells with low intensity pulsed ultrasound. Appl Phys Lett 2020;116(1):013701. https://doi.org/10.1063/1.5128627.
[220] Katiyar A, Osborn J, DasBanerjee M, Zhang LG, Sarkar K, Sarker KP. Inhibition of human breast cancer cell proliferation by low-intensity ultrasound stimulation. Ultrasound Med Biol 2020;39(10):2043–52. https://doi.org/10.1002/jum.15312.
[221] Lucchetti D, Perelli L, Colella F, Ricciardi-Tenore C, Scoarughi GL, Barbato G, et al. Low-intensity pulsed ultrasound affects growth, differentiation, migration, and epithelial-to-mesenchymal transition of colorectal cancer cells. J Cell Physiol 2020;235(6):5363–77. https://doi.org/10.1002/jcp.29423.
[222] Carina V, Costa V, Pagani S, De Luca A, Raimondi L, Bellavia D, et al. Inhibitory effects of low intensity pulsed ultrasound on osteoclastogenesis induced in vitro by breast cancer cells. J Exp Clin Cancer Res 2018;37(1):1–11. https://doi.org/10.1186/s13046-018-0868-2.
[223] Lin J, Dong S, Peng W, Liu H, Zhang P, Lv H, et al. Low-intensity pulsed ultrasound for killing tumor cells: the physical and biological mechanism. In: The proc the 16th annu conference of China electrotechnical soc. Springer; 2022. p. 812–20.
[224] Lopez W, Nguyen N, Cao J, Eddow C, Shung KK, Lee NS, et al. Ultrasound therapy, chemotherapy and their combination for prostate cancer. Technol Cancer Res Treat 2021;20:15330338211011965. https://doi.org/10.1177/15330338211011965.
[225] Singh A, Tijore A, Margadant F, Simpson C, Chitkara D, Low BC, et al. Enhanced tumor cell killing by ultrasound after microtubule depolymerization. BioEng Transl Med 2021;6(3):e10233. https://doi.org/10.1002/btm2.10233.
[226] Hoelzl MC, Fiorito M, Holub O, Fruhwirth G, Sinkus R. Oscillatory shear strain impacts metastatic cancer cell spread. Proc Int Soc Magn Reson Med 2016:2813.
[227] Glatz M. Low frequency shear waves as a potential mechanotherapy approach in cancer. Ph.D. thesis. King's College London; 2019.
[228] Hoelzl MC, Festy F, Fruhwirth G, Sinkus R. Impacting cancer cells via mechanical waves: can we change cellular behaviour? In: Proc Int Soc Magn Reson Med, vol. 20167: p. 4363.
[229] Heyden S, Ortiz M. Oncotripsy: targeting cancer cells selectively via resonant harmonic excitation. J Mech Phys Solids 2016;92:164–75. https://doi.org/10.1016/j.jmps.2016.04.016.
[230] Heyden S, Ortiz M. Investigation of the influence of viscoelasticity on oncotripsy. Comput Methods Appl Mech Eng 2017;314:314–22. https://doi.org/10.1016/j.cma.2016.08.026.
[231] Huang YL, Ma Y, Wu C, Shiau C, Segall JE, Wu M. Tumor spheroids under perfusion within a 3D microfluidic platform reveal critical roles of cell-cell adhesion in tumor invasion. Sci Rep 2020;10(1):1–11. https://doi.org/10.1038/s41598-020-66528-2.
[232] Huang D, Kidoaki S. Stiffness-optimized drug-loaded matrix for selective capture and elimination of cancer cells. J Drug Deliv Sci Technol 2020;55:101414. https://doi.org/10.1016/j.jddst.2019.101414.
[233] Jain RK, Stylianopoulos T. Delivering nanomedicine to solid tumors. Nat Rev Clin Oncol 2010;7(11):653. https://doi.org/10.1038/nrclinonc.2010.139.
[234] Polydorou C, Mpekris F, Papageorgis P, Voutouri C, Stylianopoulos T. Pirfenidone normalizes the tumor microenvironment to improve chemotherapy. Oncotarget 2017;8(15):24506. https://doi.org/10.18632/oncotarget.15534.
[235] Liu H-L, Hua M-Y, Yang H-W, Huang C-Y, Chu P-C, Wu J-S, et al. Magnetic resonance monitoring of focused ultrasound/magnetic nanoparticle targeting delivery of therapeutic agents to the brain. Proc Natl Acad Sci 2010;107(34):15205–10. https://doi.org/10.1073/pnas.1003388107.
[236] Cole AJ, Yang VC, David AE. Cancer theranostics: the rise of targeted magnetic nanoparticles. Trends Biotechnol 2011;29(7):323–32. https://doi.org/10.1016/j.tibtech.2011.03.001.
[237] Wu Y, Liu X, Qin Z, Hu L, Wang X. Low-frequency ultrasound enhances chemotherapy sensitivity and induces autophagy in PTX-resistant PC-3 cells via the endoplasmic reticulum stress-mediated PI3K/Akt/mTOR signaling pathway. OncoTargets Ther 2018;11:5621. https://doi.org/10.2147/ott.s176744.
[238] Rapoport NY, Kennedy AM, Shea JE, Scaife CL, Nam K-H. Controlled and targeted tumor chemotherapy by ultrasound-activated nanoemulsions/microbubbles. J Control Release 2009;138(3):268–76. https://doi.org/10.1016/j.jconrel.2009.05.026.
[239] Schoen Jr S, Kilinc MS, Lee H, Guo Y, Degertekin FL, Woodworth GF, et al. Towards controlled drug delivery in brain tumors with microbubble-enhanced focused ultrasound. Adv Drug Deliv Rev 2022;180:114043. https://doi.org/10.1016/j.addr.2021.114043.
[240] Tirado-Cabrera I, Martin-Guerrero E, Heredero-Jimenez S, Ardura JA, Gortázar AR. PTH1R translocation to primary cilia in mechanically-stimulated ostecytes prevents osteoclast formation via regulation of CXCL5 and IL-6 secretion. J Cell Physiol 2022. https://doi.org/10.1002/jcp.30849.
[241] Papachroni KK, Karatzas DN, Papavassiliou KA, Basdra EK, Papavassiliou AG. Mechanotransduction in osteoblast regulation and bone disease. Trends Mol Med 2009;15(5):208–16. https://doi.org/10.1016/j.molmed.2009.03.001.
[242] Dobrakowski PP, Machowska-Majchrzak AK, Łabuz-Roszak B, Majchrzak KG, Kluczewska E, Pierzchała KB. MR-guided focused ultrasound: a new generation treatment of Parkinson's disease, essential tremor and neuropathic pain. Intervent Neuroradiol 2014;20(3):275–82. https://doi.org/10.15274/inr-2014-10033.